Extratropical cyclone induced sea surface temperature anomalies in the 2013/14 winter

Helen F. Dacre [1], Simon A. Josey [2], and Alan L. M. Grant [1]

[1]University of Reading
[2]National Oceanography Centre

Correspondence: H. F. Dacre (h.f.dacre@reading.ac.uk)

Abstract. The 2013/14 winter averaged sea surface temperature (SST) was anomalously cool in the mid-North Atlantic region. This season was also unusually stormy with extratropical cyclones passing over the mid-North Atlantic every 3 days. However, the processes by which cyclones contribute towards seasonal SST anomalies are not fully quantified. In this paper a cyclone identification and tracking method is combined with ECMWF atmosphere and ocean reanalysis fields to calculate cyclone-relative net surface heat flux anomalies and resulting SST changes. Anomalously large negative heat flux is located behind the cyclones cold front resulting in anomalous cooling up to 0.2K/day when the cyclones are at maximum intensity. This extratropical cyclone induced 'cold wake' extends along the cyclones cold front but is small compared to climatological variability in the SST's. To investigate the potential cumulative effect of the passage of multiple cyclone induced SST cooling in the same location we calculate Earth-relative net surface heat flux anomalies and resulting SST changes for the 2013/2014 winter period. Anomalously large winter averaged negative heat flux occurs in a zonally orientated band extending across the North Atlantic between 40-60°N. The 2013/2014 winter SST cooling anomaly associated with air-sea interactions (anomalous heat flux, mixed layer depth and entrainment at the base of the ocean mixed layer) is estimated to be -0.67 K in the mid-North Atlantic (68% of the total cooling anomaly). The role of cyclones is estimated using a cyclone masking technique which encompasses each cyclone centre and its trailing cold front. The environmental flow anomaly in 2013/2014 sets the overall tripole pattern of heat flux anomalies over the North Atlantic. However, the presence of cyclones doubles the magnitude of the negative heat flux anomaly in the mid-North Atlantic. Similarly, the environmental flow anomaly determines the location of the SST cooling anomaly but the presence of cyclones enhances the SST cooling anomaly. Thus air-sea interactions play a major part in determining the extreme 2013/2014 winter season SST cooling anomaly. The environmental flow anomaly determines where anomalous heat flux and associated SST changes occur and the presence of cyclones influences the magnitude of those anomalies.

1 Introduction

The interaction of the ocean and atmosphere has long been recognised as an important element of oceanic cyclogenesis. In the tropics, sub-saturation of air above the sea surface in the vicinity of tropical cyclones results in strong surface heat flux which cools the upper ocean in the wake of tropical cyclones (Kleinschmidt, 1951; Fisher, 1958). In addition, strong winds

enhance mixing in the upper-ocean, which can result in the transport of cool water to the surface. Similarly, in the mid-latitudes it was observed by Pettersen et al. (1962) that surface heat fluxes are largest in the advancing cold air mass behind an extratropical cyclone's cold front. Although fluxes are typically an order of magnitude smaller in extratropical cyclones than tropical cyclones, they still have the potential to influence the underlying ocean.

Alexander and Scott (1997) analyzed the association of ocean heat fluxes with propagating extratropical cyclones on synoptic timescales. They found increased fluxes directed from the ocean to the atmosphere in the western parts of the cyclones and the eastern parts of the cyclones were associated with decreased fluxes directed from the ocean to the atmosphere. These results have been confirmed by many subsequent studies (Persson et al., 2005; Nelson et al., 2014; Schemm and Sprenger, 2015; Dacre et al., 2019) and suggest a close association between the cyclones and surface turbulent fluxes in the midlatitudes. However, a cyclone compositing study by Rudeva and Gulev (2011) found that although composites of fluxes show locally very strong positive fluxes in the rear part of the cyclone, the total air-sea turbulent fluxes provided by cyclones were not significantly different from the averaged background fluxes in the North Atlantic suggesting at least partial cancellation of the flux anomalies associated with cyclones.

The anomalous surface heat fluxes generated by cyclones can create SST anomalies known as the 'cold wake' effect. Case studies of winter cyclones in the North-West Atlantic have found SST cooling in the rear part of cyclones of between 0.4 and 2 K (Ren et al., 2004; Nelson et al., 2014; Kobashi et al., 2019). This is largely due to enhanced turbulent fluxes behind the cold front, however Kobashi et al. (2019) also attribute part of the cooling to cloud shielding of incoming solar radiation, although this is possibly due to the more southerly latitude of the cyclone in their study. Cooling may also result from an episodic wind effect, known as resonant wind-driven mixing, which occurs when the rotation rate of the winds at a fixed point matches the rotation of the wind driven currents (Crawford and Large, 1996). The magnitude of the cooling has been shown to depend on the cyclone's intensity (Yao et al., 2008; Rudeva and Gulev, 2011) with stronger cyclones creating enhanced surface fluxes and hence increased cooling. In addition, there is some seasonality in the cooling magnitude, with largest cooling occurring in late summer and autumn when the ocean surface mixed layer in the Northern Hemisphere is shallower (Ren et al., 2004; Kawai and Wada, 2011). Finally, the relationship between enhanced turbulent fluxes is regionally dependent. For example, Tanimoto et al. (2003) showed that in the central North Pacific, enhanced turbulent fluxes can generate local SST variations but in regions where ocean dynamics are important, such as the western Pacific, the SST anomalies formed in the early winter determine the mid- and late-winter turbulent heat flux anomalies rather than the passage of cyclones. Similarly, Buckley et al. (2015) find that in the Gulf Stream region, ocean dynamics are important in setting the upper-ocean heat content anomalies on interannual time scales and that air–sea heat fluxes damp anomalies created by the ocean.

The effect of extratropical cyclone induced fluxes on longer timescale variability has been investigated in both the Atlantic and Pacific. Several studies have shown that wintertime fluxes in the Gulf Stream are characterized by episodic high flux events due to cold air outbreaks from North America associated with the passage of extratropical cyclones (Zolina and Gulev, 2003; Shaman et al., 2010; Parfitt et al., 2016, 2017; Ogawa and Spengler, 2019). Similar relationships have been found in the high-latitude South Pacific by Papritz et al. (2015). The influence of these enhanced fluxes is to restore the low-level atmospheric

baroclinicity destroyed by the passage of the cyclones (Vannière et al., 2017) but the impact on the underlying SST's has not been quantified.

While the role of individual cyclones on local SST's have been studied, the cumulative effect of cyclone induced SST changes over individual seasons has not received much attention in the literature. During the winter of 2013/2014 a cold anomaly developed in the SST in the mid Atlantic. Grist et al. (2016) found that during this winter enhanced sensible and latent heat fluxes occurred in the North Atlantic, with latent heat fluxes being largest in the east North Atlantic and sensible heat flux anomalies stronger in the west North Atlantic resulting in a reduction in ocean heat content of the subpolar gyre. The extent to which extratropical cyclones were responsible for these enhanced fluxes and associated cooling is not well understood.

In this paper we investigate both the SST cooling associated with individual cyclones and the SST cooling associated with the passage of multiple cyclones over the same location in the 2013/2014 season to determine how significant cyclones were in contributing to the observed cooling.

2 Data and Analysis Methods

2.1 ERA-Interim data

ERA-Interim is a global atmospheric reanalysis dataset (Dee et al., 2011). The data assimilation system used to produce ERA-Interim is based on Integrated Forecasting System (Cy31r2). The system includes a 4-dimensional variational analysis with a 12 hour analysis window. The spatial resolution of the data set is approximately 80 km (T255 spectral) on 60 vertical levels from the surface up to 0.1 hPa. 6 hourly ERA-Interim data has been used in this study to determine extratropical-cyclone related SST changes. We analyse several re-analysis fields from ERA-Interim which are described in this section.

The net surface thermal radiation (Q_{LW}) is the thermal radiation emitted by the atmosphere and clouds reaching the surface minus the amount emitted by the surface. Surface solar radiation (Q_{SW}) is the amount of solar radiation reaching the surface (both direct and diffuse) minus the amount reflected by the surface. Surface latent heat flux (Q_E) is the exchange of latent heat with the surface through turbulent diffusion and the surface sensible heat flux (Q_H) is the exchange of sensible heat with the surface. The magnitudes of Q_E and Q_H depend on the windspeed and moisture and temperature differences between the surface and the lower atmosphere.

The net surface heat flux (Q_N) is given by the sum of Q_{SW}, Q_{LW}, Q_H and Q_E. The ECMWF convention for vertical fluxes is positive downwards. We also analyse ERA-Interim SST's which are the temperatures of sea water near the surface. ERA-Interim SST's are taken from different sources depending on the dates of the reanalyses: NCEP 2D-Var SST (Jan 1989 – Jun 2001); NOAA Optimum Interpolation SST v2 (Jul 2001 – Dec 2001); NCEP Real-Time Global SST (Jan 2002 – Jan 2009); Met Office Operational SST (Feb 2009 - 2015).

2.2 ECMWF Ocean Reanalysis System (ORAS5)

The ECMWF Ocean Reanalysis System 5 (ORAS5) is a global eddy-permitting ocean-sea ice reanalysis system. It provides an estimate of the historical ocean state from 1979 to present. The ocean model resolution in ORAS5 is 0.25 degree in the horizontal (approximately 25 km in the tropics, and increasing to 9 km in the Arctic) and 75 levels in the vertical. ORAS5 uses the Nucleaus for European Modelling of the Ocean (NEMO v3.4.1) ocean coupled to the Louvain-la-Neuve Sea Ice Model (LIM2) sea-ice model. It includes a prognostic thermodynamic-dynamic sea-ice model with assimilation of sea-ice concentration data (Zuo et al., 2017, 2019). The ocean mixed layer is the layer immediately below the ocean air-sea interface and is typically tens of meters deep in summer while values of several hundred meters may be reached in winter. In this paper the interannually and monthly varying mixed layer depth (MLD) from ORAS5 is used to calculate the SST tendencies (ΔSST) due to surface heat flux between 1989-2016. The ORAS5 MLD is the first depth at which the density difference, compared to density at 10 m depth, reaches 0.01kg/m^3. The Ocean Reanalysis MLD agrees well with the observationally based MLD estimates in the mid-Atlantic (Toyoda et al., 2017). However, in deep convective regions, such as the Labrador Sea, the density difference MLD definition can overestimate MLD (Courtois et al., 2017).

2.3 Cyclone identification

Following Dacre et al. (2012) we identify and track the position of the 200 most intense cyclones in 20 years of the ERA-Interim dataset (1989-2009) during wintertime only (DJF) using the tracking algorithm of Hodges (1995). Tracks are identified using 6-hourly 850 hPa relative vorticity, truncated to T42 resolution to emphasize the synoptic scales. The 850 hPa relative vorticity features are filtered to remove stationary or short-lived features that are not associated with extratropical cyclones. The intensity of the cyclones is measured by the maximum T42 vorticity. The 200 most intense DJF cyclone tracks with maximum intensity in the North Atlantic ($70° - 10°$ W, $30° - 90°$ N) are used in this study and they account for 19% of the total number of identified North Atlantic cyclone during this period. These tracks are shown in figure 1(a). The cyclones generally propagate in a north-easterly direction, from the east coast of America towards Iceland. The position of the cyclones 24 hours before maximum intensity (*max -24*) are predominantly over the Gulf Stream (figure 1(b)). By maximum intensity (*max*) the majority of cyclones are located east of Newfoundland (figure 1(c)). During the decaying stage of the cyclones evolution (*max + 24*) the cyclones are more uniformly distributed across the North Atlantic (figure 1(d)).

2.4 Cyclone-relative composites

The fields, described in section 2.1, are extracted from ERA-Interim at each of the 6 hourly locations of the cyclone within a $30°$ radius surrounding the cyclone centre. Cyclone-relative composites are produced by averaging over all cyclones. Following Catto et al. (2010), before compositing the fields are rotated according to the direction of travel of each cyclone such that the direction of travel in the composite becomes the same for all cyclones. Since the cyclones have quite different propagation directions, performing the rotation ensures that mesoscale features such as warm and cold fronts are approximately aligned and are not smoothed out by the compositing. As this method assumes that the cyclones all intensify and decay at the same rate

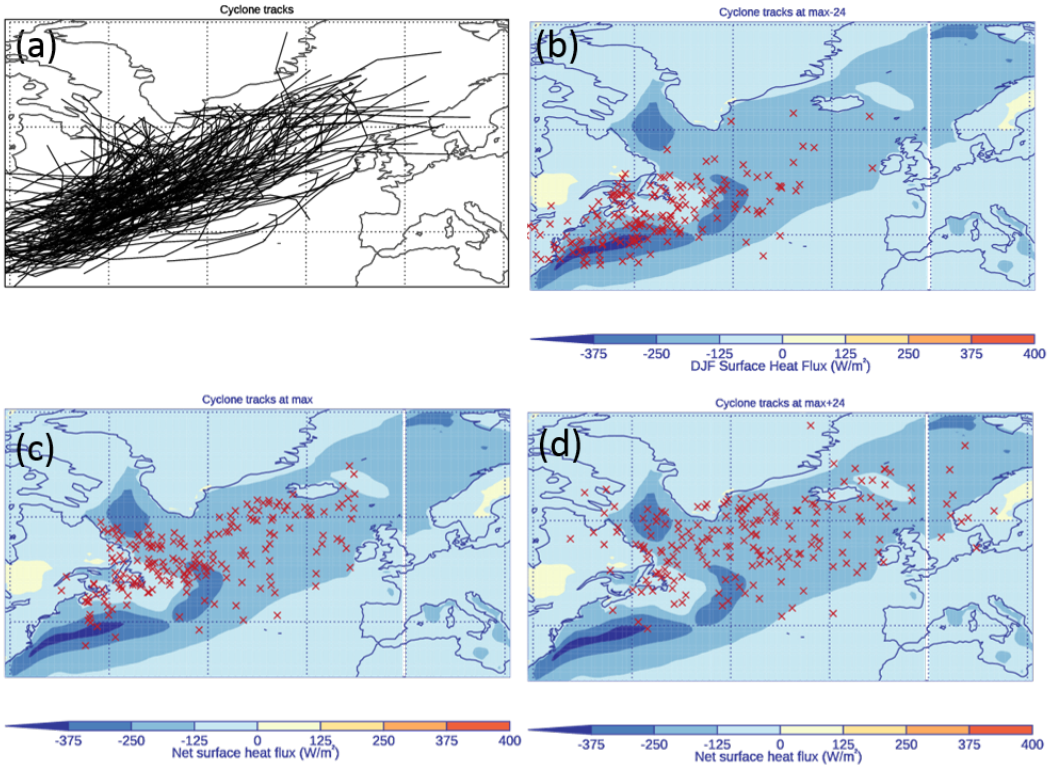

Figure 1. (a) Tracks of the 200 most intense DJF North-Atlantic storms between December 1989 and February 2009 (black). Position of the cyclones (b) 24 hours before maximum intensity (max-24), (c) at maximum intensity (max) and (d) 24 hours after maximum intensity (max+24) (red crosses). Overlaid on the DJF North Atlantic 1989-2015 net surface heat flux climatology, Q_N (W/m^2).

only the 200 most intense cyclones are included in the composite. The 850 hPa relative vorticity mean and standard deviation of the of these cyclone are shown in Dacre et al. (2012) (their figure 2(c)). Limiting the number of cyclones produces a more homogeneous group in terms of their evolution but will bias the mean fields to be typical of the most intense cyclones. Data are only included in the composite where grid points lie over ocean surface.

2.5 Cyclone and environmental flow partition

To understand the part played by cyclones in the development of the cold anomaly during the winter of 2013/2014 the net surface heat flux is partitioned into environmental and cyclone components. To partition Q_N into a part due to environmental flow and a part associated with cyclones we combine the cyclone tracks for that season with a masking method. A cyclone mask is calculated for each time step where the regions influenced by a cyclone are given a value of one (i.e., they are inside the cyclone mask) and regions that are not influenced are given a value of zero (i.e., they are outside the cyclone mask) (Hawcroft et al., 2012; Sinclair and Dacre, 2019). The heat flux associated with cyclones are asymmetric around the cyclone.

Large negative flux is found close to the cyclone centre and extending along the trailing cold front which lies to the west of the cyclone centre. To account for this, a cyclone mask at a given time, t, is created by identifying the position of a cyclone and also it's position during the previous 30 hours. A mask is created which extends 14° in a radial circle from each track point, creating an elongated oval shape which encompasses both the cyclone centre and the elongated cold front (figure 2). This is equivalent to taking a swath with circles around all cyclone positions in the previous 30 hours. The Q_N anomaly when

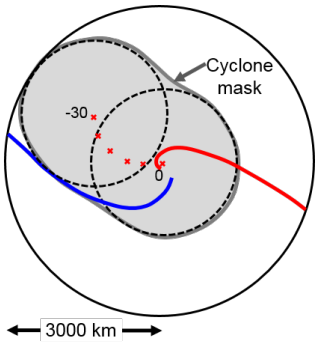

Figure 2. Schematic of cyclone masking method. Red and Blue lines show the approximate position of the cyclone warm and cold front respectively. Red crosses show the position of a given cyclone at time (t) and at 6-hourly intervals up until 30 hours previously (-30). The outer circle shows the 30 degree radius circle used to produce the composites in figures 5 to 8. The smaller dashed circles show example locations of a 14 degree radius circle centred on the cyclone position at t=0 and t=30. The grey shading shows the extent of the cyclone mask.

cyclones are not present is associated with the environmental flow. The Q_N anomaly within the cyclone masks is associated with cyclones embedded within the environmental flow.

2.6 Sea Surface Temperature Tendency

In order to calculate the SST tendency (ΔSST) we must take into account the mixed layer depth (MLD) through which the heating or cooling due to the surface fluxes is mixed (h). Mixing in the ocean is assumed to occur between the surface and the MLD obtained from ORAS5. Assuming a well-mixed layer, the SST tendency due to Q_N and MLD (ΔSST_{Q_N}) is given by;

$$\Delta\text{SST}_{Q_N} = \frac{1}{\rho c_p}\frac{Q_N}{h}, \tag{1}$$

where ρ is the density of sea water, 1024kgm^{-3}; c_p is the specific heat capacity of sea water, $4000\text{Jkg}^{-1}\text{K}^{-1}$.

The SST tendency anomaly, $\Delta SST^{'}$, for the 2013/2014 season is determined by subtracting the climatological SST tendency from the 2013/2014 SST tendency. The SST tendency anomaly can be separated into the anomaly associated with (i) anomalous Q_N (term 1 in equation 2), (ii) anomalous MLD (term 2 in equation 2) and (iii) anomalous entrainment through the base of the mixed layer, Q_{ENT} (term 3 in equation 2). We refer to the sum of these quantities as the SST tendency anomaly due to air-sea

interactions (ASI), $\Delta\text{SST}'_{ASI}$, given by;

$$\Delta\text{SST}'_{ASI} = \frac{Q_N^i - \overline{Q_N}}{\rho c_p \overline{h}} + \frac{Q_N^i}{\rho c_p}\left(\frac{1}{h^i} - \frac{1}{\overline{h}}\right) + \frac{Q_{ENT}^i - \overline{Q_{ENT}}}{\rho c_p \overline{h}}, \quad (2)$$

where the overbar represents the 1989-2015 climatological value. Since we have no measurements of the entrainment flux anomaly across the ocean boundary layer it is estimated to be 20% of the surface Q_N anomaly (Stull, 1988). This estimate for the entrainment flux neglects contributions made by wind-driven turbulence.

3 Results

3.1 North Atlantic heat flux and SST tendency climatologies

Figure 3 shows the average heat flux for the period DJF 1989-2015 over the North Atlantic. The net surface solar radiation is positive with a meridional gradient of 50 $\text{Wm}^{-2}1000\text{km}^{-1}$ (figure 3(a)) and the net thermal radiation (figure 3(b)) is negative with a magnitude between -50 and -100 Wm^{-2}. The sensible heat flux (figure 3(c)) is generally positive over land and negative over the ocean with negative flux between -50 and -150 Wm^{-2} in the Gulf Stream and Davis Strait regions caused by the advection of cold air from the land over relatively warm oceans in DJF. The latent heat flux (figure 3(d)) is generally negative, with a band of enhanced negative flux extending in a north-eastwards direction from the east coast of the US towards Iceland with the values > 200 Wm^{-2} found in the west of the North Atlantic. The net heat flux, Q_N, (figure 3(e)), is negative over the majority of the domain. A combination of Q_H and Q_E results in maximum negative heat flux > 300 Wm^{-2} in the Gulf Stream region. The largest Q_N are co-located with the position of the North Atlantic storm track (figure 3(f)) which also exhibits a pronounced south-west to north-east tilt similar to the storm track in figure 1(a).

Figure 4(a) and (b) show the climatological SST and the average SST change over DJF (ΔSST_{TOT}) for the period 1989-2015. During DJF the North Atlantic cools by an average of 2K (figure 4(b)). The cooling is greatest where the SST gradient is largest in the Gulf Stream region (dotted box in figure 4(a)), with cooling of over 6 K over the winter. Unlike the climatological Q_N shown in figure 3(e) the region of highest ΔSST_{TOT} does not extend over the North Atlantic towards Iceland but remains close to the east coast of the US.

In order to calculate the SST tendency due to Q_N we must take into account the mixed layer depth (MLD) through which heating or cooling at the surface is mixed using equation 1. Figure 4(c) shows the climatological MLD. The MLD ranges from a few 10s of metres close to Newfoundland, to over 1000m in the Labrador and Norwegian seas where deep convection occurs. On average the MLD deepens by 50% between December and February outside the deep convection regions (not shown). Taking the MLD into account restricts the largest ΔSST_{Q_N} to the western North Atlantic region (figure 4(d)). The difference between ΔSST_{TOT} and ΔSST_{Q_N} is shown in figure 4(e). Differences > 6K are found close to the coast where the western boundary currents transport warm waters north resulting in reduced cooling over the DJF period than would be expected due to Q_N alone.

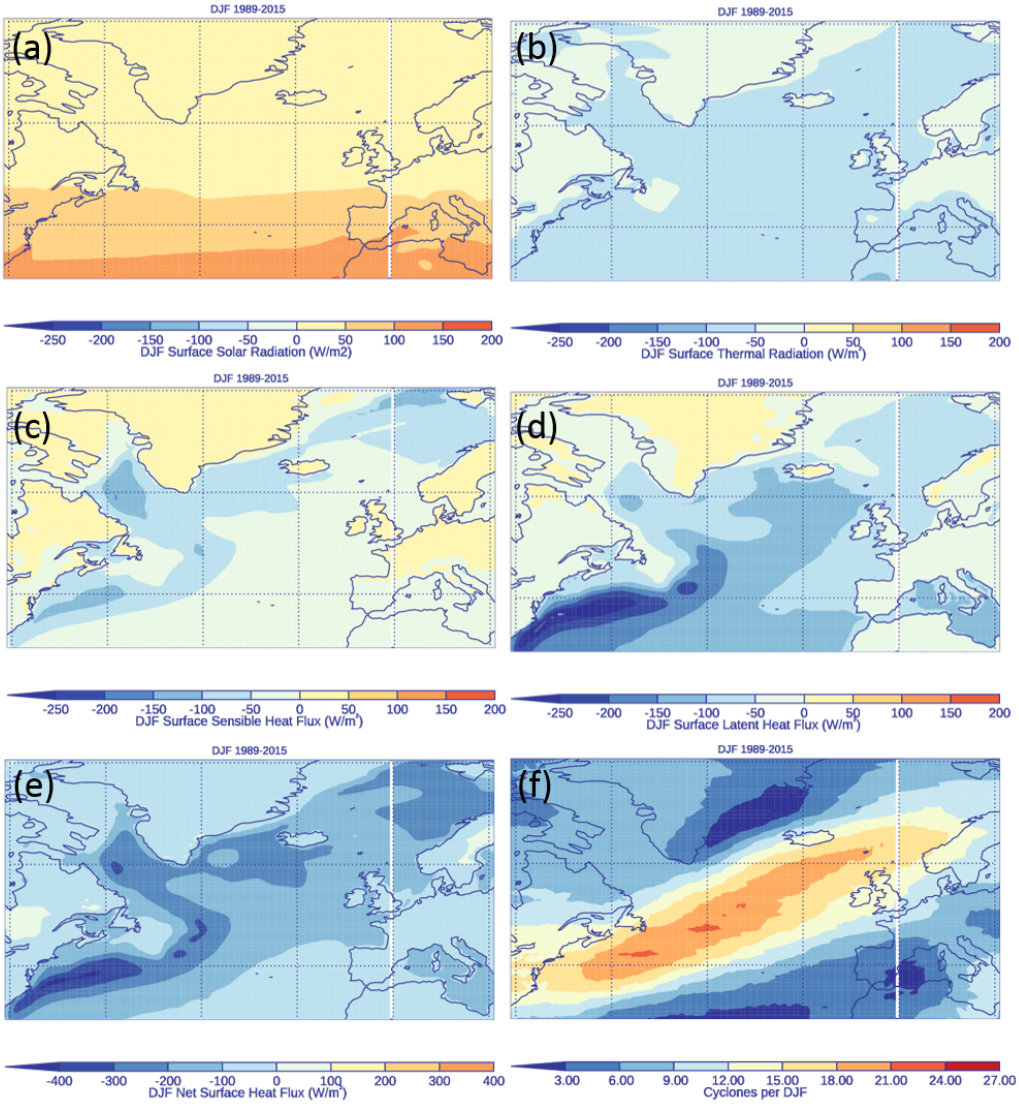

Figure 3. North Atlantic 1989-2015 heat flux climatologies (W/m^2). (a) Surface solar radiation Q_{SW}, (b) surface thermal radiation Q_{LW}, (c) surface sensible heat flux Q_H, (d) surface latent heat flux Q_E and (e) net surface heat flux Q_N. Note change in scale in figure (e). Positive flux is into the surface and negative flux is into the atmosphere. (f) 1989-2015 climatological number of cyclones per DJF season within 12° of grid point.

3.2 Cyclone-relative heat flux composites

The north-south SST gradient in figure 4(a) is important for creating negative heat flux when cold dry air, from higher latitudes, is advected over relatively warm ocean surfaces. The largest heat flux occurs when large differences in temperature or moisture between the surface and overlying atmosphere are co-located with enhanced wind speeds. Given the spatial distribution of

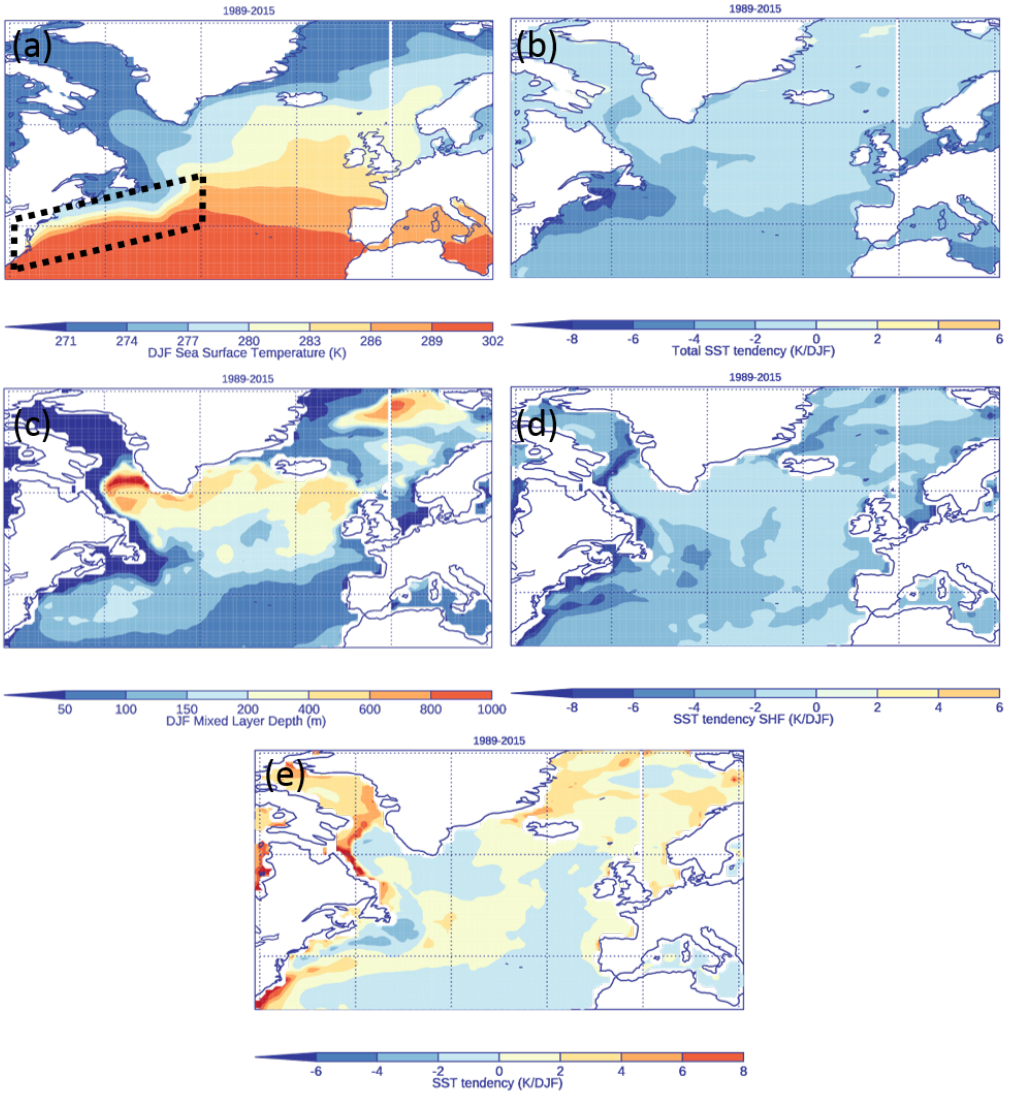

Figure 4. North Atlantic DJF 1989-2015 (a) sea surface temperature (SST, K), black dotted box outlines region of the Gulf Stream, (b) ΔSST_{TOT} (K/DJF), (c) mixed layer depth (m), (d) ΔSST_{Q_N} (K/DJF), (e) Difference between ΔSST_{TOT} and ΔSST_{Q_N}.

SST's, atmospheric temperatures and moisture content, this is likely to occur when there are anomalously strong meridional winds such as found ahead of and behind extratropical cyclones. Thus, whilst the maximum climatological SST gradient controls where locally high surface flux occurs, the presence of extratropical cyclones are likely to control when the largest heat flux occurs and its magnitude (Rudeva and Gulev, 2011; Ogawa and Spengler, 2019). In addition, the similarities between the spatial pattern of climatological Q_N (figure 3(e)) and cyclone numbers per season (figure 3(f)) suggests that cyclones play

a role in generating Q_N. In this section we investigate Q_N in a cyclone-relative frame of reference using the methodology described in sections 2.3 and 2.4.

Figure 5 shows composite cyclone centred heat flux for the 200 most intense cyclones occurring between 1989-2009. The cyclones are at maximum intensity (maximum 850 hPa relative vorticity) when they are located at the centre of the domain and have been rotated so that they all travel from left to right. Q_{SW} (figure 5(a)) contribution to Q_N is positive and, like the Earth-relative perspective (figure 3(a)), there is a weak gradient. However, because the cyclones are typically travelling in a north-eastwards direction and they have been rotated, this gradient is also rotated. Q_{LW} (figure 5(b)) is negative everywhere and small, similar to the Earth-relative perspective. Q_{LW} is slightly enhanced in the region behind the cold front, potentially due to a reduction of cloud, which reduces the downwelling radiation. Q_H (figure 5(c)) shows a dipole structure at this stage in the cyclones evolution, with negative flux behind the cyclone centre and positive flux in the cyclones' warm sector. Q_E (figure 5(d)) is negative everywhere, a minimum in an extended region behind the cyclone and reduced ahead of the cyclone. Q_N (figure 5(e)) is therefore negative surrounding the cyclone centre with a minimum behind the cyclone. Negative flux > 200 W/m^2 occurs within 1000 km of the cyclone centre but extend almost 2000 km behind the cyclone due to a combination of Q_H and Q_E occurring behind the cold front.

In order to illustrate the processes leading to negative Q_H behind the cyclone cold front and positive Q_H in the warm sector it is necessary to examine the temperature characteristics of the different airmasses in these regions. Figure 6(a) shows the composite 10 m air temperature overlaid with 925 hPa winds and figure 6(b) shows the SST. The 10 m air temperature exhibits a wave like structure whilst the SST gradient is more linear. This results in a large negative near surface temperature difference (SST $>$ 10 m temperature) behind the cold front. Cyclonic winds advect relatively cold air over a warm ocean surface behind the cyclone resulting in negative Q_H. Ahead of the cyclone cyclonic winds advect warm air over the ocean surface. 6 hours before maximum intensity the SST $<$ 10m air temperature ahead of the cyclone (not shown) but at maximum intensity the difference is close to zero (white contour in figure 6(b) shows -0.4 K). Since Q_H is a 6-hour average, this results in the positive Q_H observed in figure 5(c). Figure 6(d) and (e) show the 10 m specific humidity and the saturation specific humidity at the SST respectively. The 10 m specific humidity also has a pronounced wave structure with drier air behind the cold front and moister air in the warm sector. Behind the cold front the saturation deficit is > 4 g/kg (figure 6(f)) causing evaporation of moisture from the surface and large negative Q_E observed in figure 5(d). Ahead of the cyclone the moisture deficit is < 1 g/kg significantly reducing the magnitude of Q_E.

Figures 7(a)-(c) show composite Q_N centred on cyclones at different stages in their evolution. As the cyclones start to intensify negative Q_N behind the cold front strengthens (figure 7(b)). During the mature stages of the cyclone evolution (figure 7(c)) Q_N begins to decrease and to wrap cyclonically around the cyclone centre. This is due to the fact that the cold front typically rotates cyclonically towards the warm front as the cyclone reaches maturity. These results are consistent with the findings of Rudeva and Gulev (2011) who found that turbulent heat flux increases with cyclone intensity.

Interestingly, throughout the cyclone lifecycle there is a secondary minimum in Q_N occurring approximately 2000 km ahead of the cyclone location. This secondary minima does not change magnitude so is unlikely to be affected by the cyclones at the

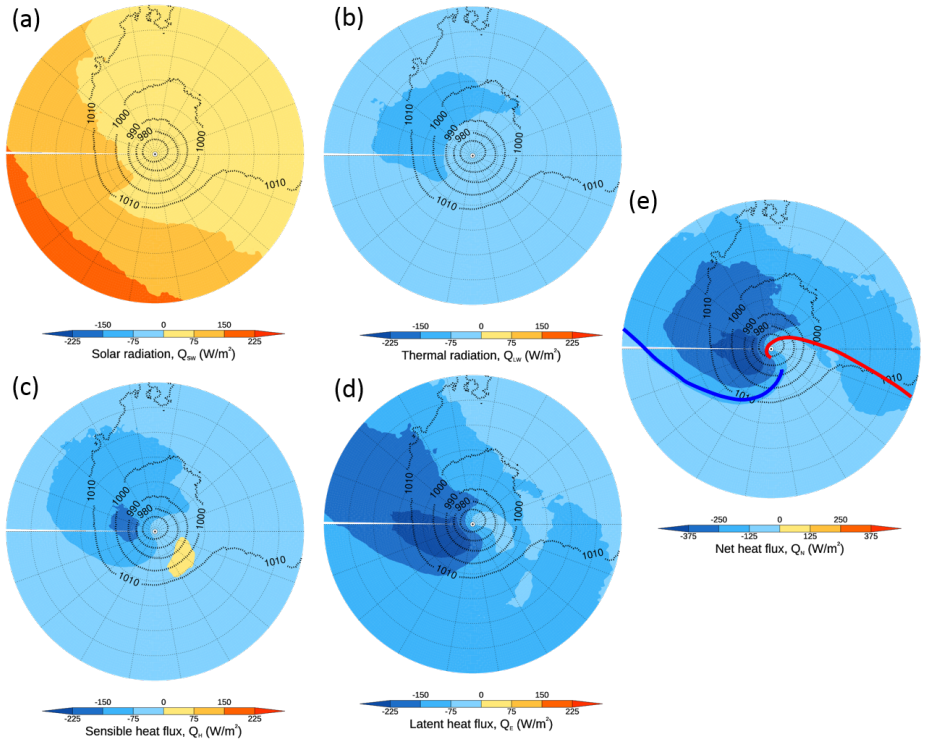

Figure 5. Composite cyclone centred heat fluxes (W/m^2) for cyclones at maximum intensity. (a) Surface solar radiation Q_{SW}, (b) surface thermal radiation Q_{LW}, (c) surface sensible heat flux Q_H, (d) surface latent heat flux Q_E and (e) net surface heat flux Q_N overlaid with mslp. Note the change in colour scale in figure (e). Positive fluxes are into the surface and negative fluxes are into the atmosphere. The radius of the circles is 3000 km and the cyclones are travelling from left to right. The blue and red lines in (e) represent the approximate positions of the cold and warm fronts at max intensity.

centre of the composite. It is possible that this second minima is due the presence of a downstream cyclone indicated by the composite mslp contours, which extend towards the upper-right quadrant of the domain.

Since many of the 200 cyclones contributing to the composite Q_N (figure 5(e)) are generated over the Gulf-Stream region it is possible that large negative Q_N occurring behind of the cyclone centre could be an artifact of their preferential cyclogenesis over a region of climatologically large negative Q_N (figure 3(e)). To determine how Q_N compares to the background values we normalise Q_N anomalies by subtracting the climatological field at the position of each cyclone and divide by the standard deviation of the climatology at the same location. Figures 7(d)-(f) show normalised Q_N anomalies at different stages of the cyclone evolution. Negative anomalies indicate anomalously large heat flux into the atmosphere, with a value of -1 being 1 standard deviation larger than the climatological mean. Positive anomalies indicate anomalously small heat flux into the atmosphere, with a value of +1 being 1 standard deviation smaller than the climatological mean. At all stages of the cyclone evolution negative Q_N behind the cyclone centre is more than 0.5 standard deviations greater than the mean for strong cyclones

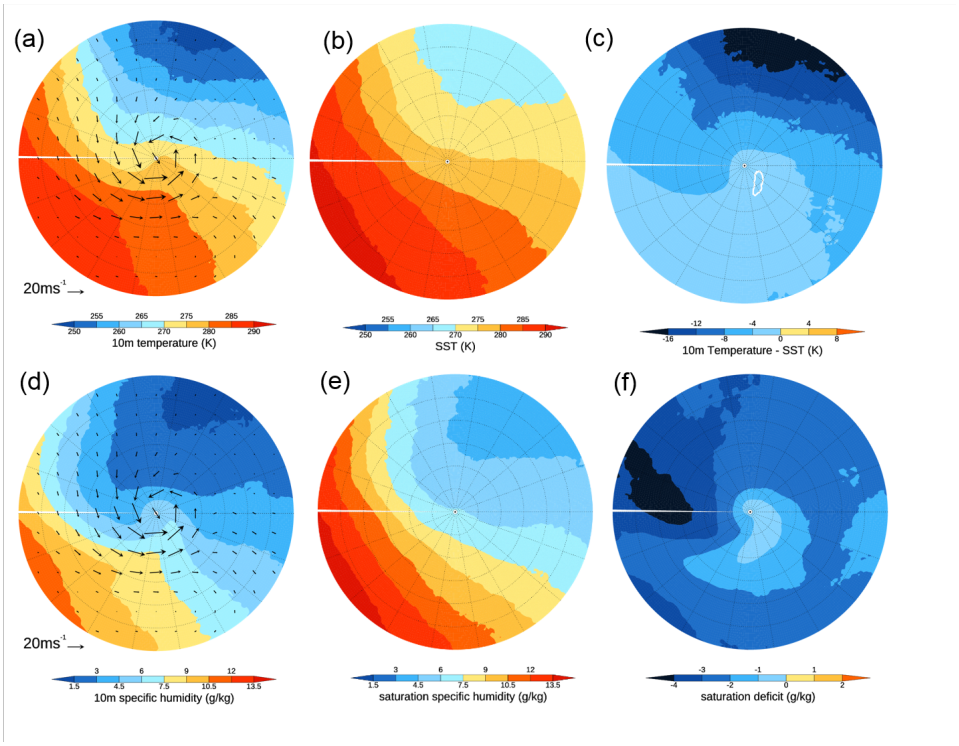

Figure 6. Cyclone centred fields at maximum intensity. (a) 10m air temperature (K), (b) SST (K), (c) 10m temperature - SST (white contour is -0.4 K) (K), (d) 10m specific humidity (g/kg), (e) saturation humidity of SST (g/kg), (f) 10m specific humidity - saturation humidity of SST (g/kg). (a) and (d) overlaid with 925hPa winds.

and is more than 1 standard deviations greater than the mean at maximum intensity (figure 7(e)). Ahead of the cyclone Q_N is $0.4 - 0.8$ standard deviations greater than the mean at maximum intensity (figure 7(e)) due to warm air advection in the warm sector of the cyclone. Note that towards the edges of the domain many of the gridpoints are over land so have been excluded, therefore the sample size contributing to the composites is small resulting in noisy field.

3.3 Cyclone-relative SST tendency

Using equation 1 the evolution of the cyclone-relative SST tendencies due to Q_N can be estimated. Figure 8 shows ΔSST_{Q_N} per day for cyclones at different stages in their evolution. The patterns of ΔSST_{Q_N} are similar to the patterns of Q_N (figure 7(a)-(c)) showing that the surface flux is the dominant variable in the cooling and that variations in mixed layer depth are less important. As for Q_N, ΔSST_{Q_N} increases as the cyclones reach maximum intensity with maximum SST tendencies of 0.2K/day occurring in the cold sector behind the cold front. The normalised ΔSST_{Q_N} anomalies are calculated by subtracting the climatological ΔSST_{TOT} and dividing by the standard deviation of ΔSST_{TOT} (figures 8(d)-(f)). ΔSST_{Q_N} is larger than

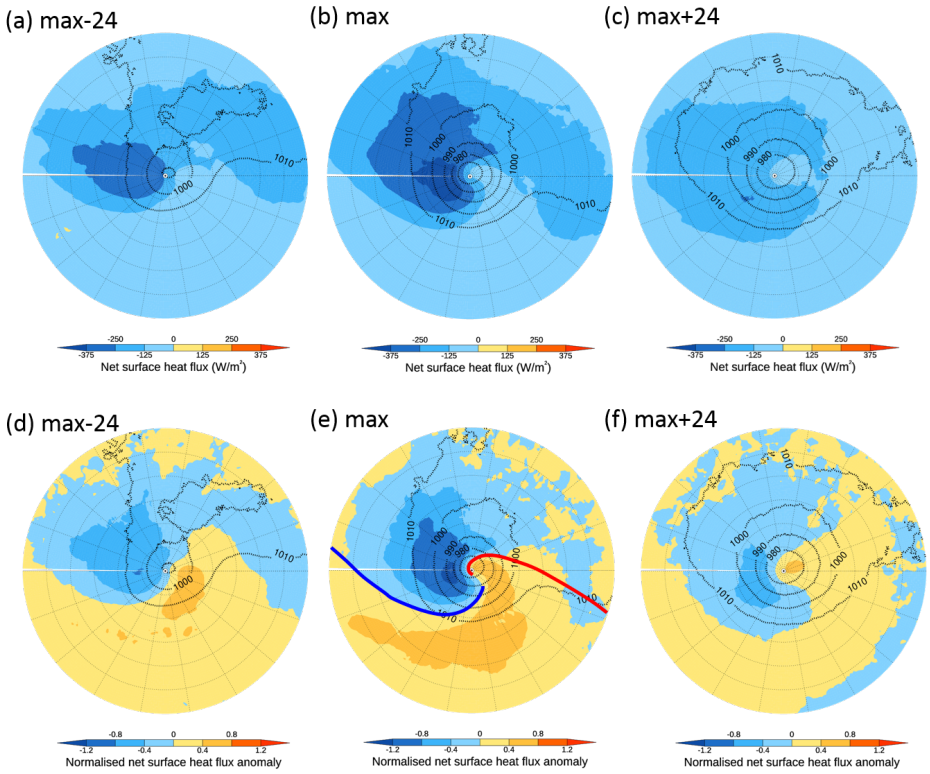

Figure 7. Evolution of cyclone centred (a)-(c) net surface heat flux Q_N (filled contours, W/m^2), (d)-(f) normalised net heat flux anomaly (filled contours) and mslp (black contours, hPa). Cyclones reach the centre of the domain (a),(d) 24 hours before maximum intensity, (b),(e) at maximum intensity and (c),(f) 24 hours after maximum intensity. In (d)-(f) negative normalised heat flux anomalies indicate anomalously large heat flux into the atmosphere and positive anomalies indicate anomalously small heat flux into the atmosphere compared to climatology. The blue and red lines in (e) represent the approximate positions of the cold and warm fronts at max intensity.

the climatological mean behind the cold front. However in this case the intense cyclones only reduce ΔSST by up to 0.25 times the standard deviation.

4 2013/2014 heat flux anomalies

ΔSST_{Q_N} cooling associated with each individual extratropical cyclone is of the order $0.1-0.2$K/day (figures 8(a)-(c)) therefore if many cyclones track over the same location we might expect to see a signature of the storm track in the seasonal Q_N and SST anomaly patterns. Figure 9(a) shows the tracks of cyclones in the North Atlantic region. Applying the cyclone masking methodology described in section 2.6 to the 2013/2014 winter cyclones we see that the cyclones track in a south-west to north-east direction in a narrow band that extends from the east coast of the US towards the UK (figure 9(b)). This season was unusually stormy in the UK with cyclones passing over the UK every 3 days (Priestley et al., 2017). The effect of propagation

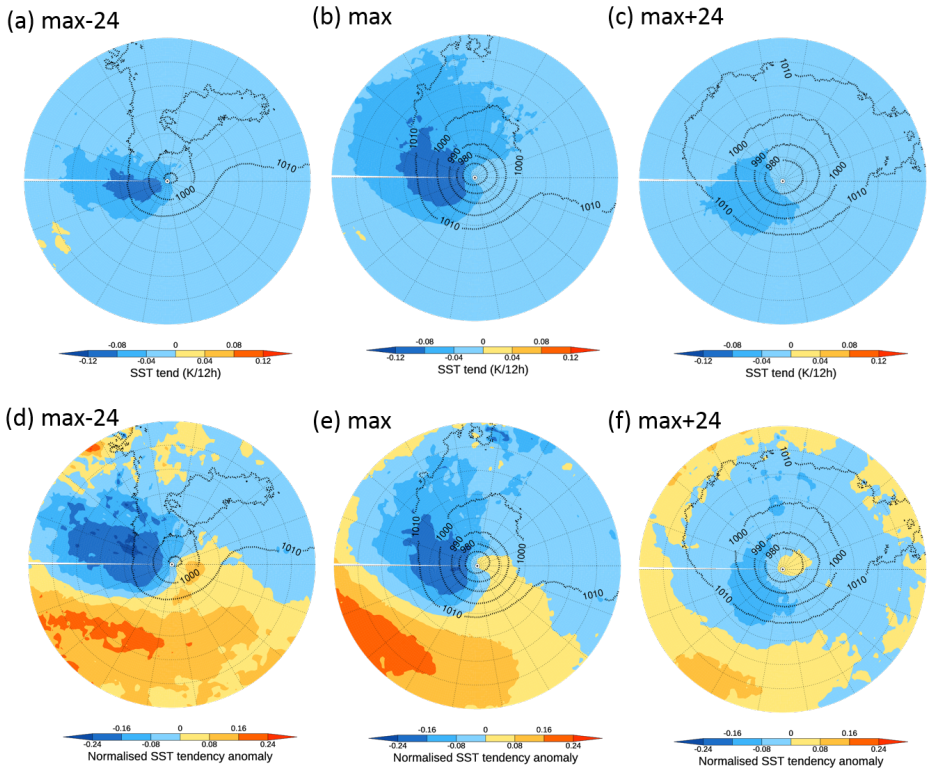

Figure 8. Evolution of cyclone centred (a)-(c) ΔSST_{Q_N} (filled contours, K/day), (d)-(f) Normalised ΔSST_{Q_N} anomaly (filled contours) and mslp (black contours, hPa). Cyclones reach the centre of the domain (a),(d) 24 hours before maximum intensity, (b),(e) at maximum intensity and (c),(f) 24 hours after maximum intensity. In (d)-(f) Negative normalised ΔSST_{Q_N} anomalies indicate anomalously large SST cooling due to Q_N and positive anomalies indicate anomalously small SST cooling compared to climatology.

speed is taken into account in the masking methodology since multiple timesteps for a single cyclone contribute to the seasonal mask fraction. We also apply the cyclone masking methodology to winter cyclones between 1989-2015 (figure 9(c)) and find that, in comparison to the 1989-2015 average, the 2013/2014 the storm track was more active, with a higher number of cyclones and also more zonal than usual (figure 9(d)). This was associated with an anomalously strong and zonally elongated upper-level westerly jet in 2013/2014 (Kendon and McCarthy, 2015). More cyclones travelled towards western Europe than Iceland than usual.

It was shown in figure 7 that intensifying cyclones create negative Q_N behind the cold front, where cold dry air is advected over a warm ocean surface. Therefore we hypothesise that an anomalously strong and zonal storm track will result in an anomalously strong and zonally orientated seasonal Q_N anomaly. The 2013/2014 DJF season Q_N is shown in figure 9(e) and the 2013/2014 Q_N anomaly shown in figure 9(f). The seasonal Q_N anomaly has a tripole pattern, with stronger negative Q_N in the mid-North Atlantic and weaker negative Q_N over the Gulf Stream and in the Norwegian and Greenland Seas. In the

mid-Atlantic this is consistent with the shift in the storm track, with cyclones travelling more zonally from the US towards western Europe rather than north-eastwards towards Iceland.

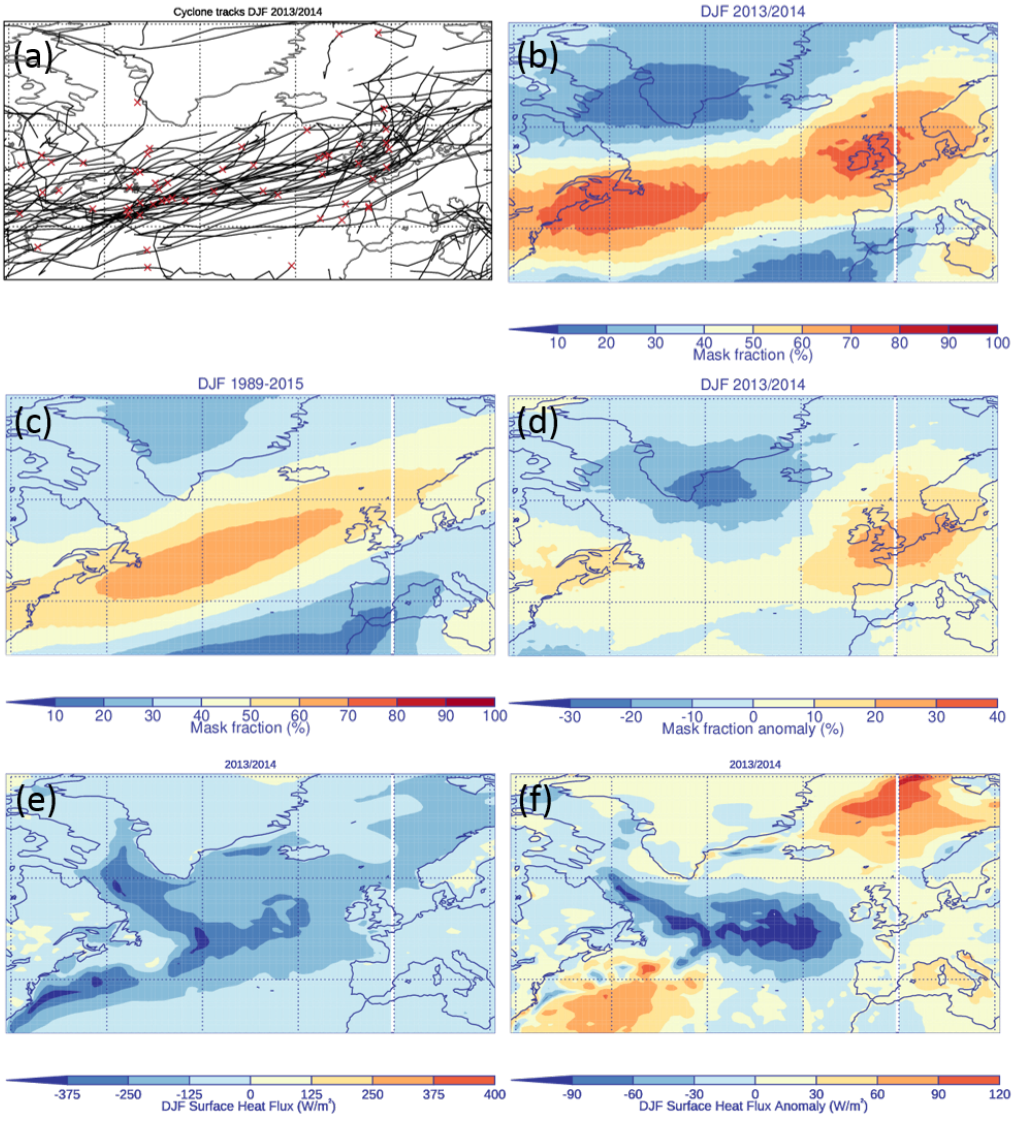

Figure 9. (a) 2013/2014 cyclone tracks (black) with position of maximum intensity (red crosses), (b) 2013/2014 fraction of time within cyclone mask, (c) 1989-2015 mask fraction, (d) anomalous mask fraction, (e) 2013/2014 Q_N (W/m^{-2}) and (f) anomalous Q_N (W/m^2).

Figures 10(a) and (b) show UK Met Office synoptic analysis charts at 00UTC on 24 and 20 December 2013 respectively. At both times there is a low pressure centre situated to the west of Scotland and long trailing cold fronts extending across the north Atlantic. Figures 10(c) and (d) show Q_N at the corresponding times and figures 10(e) and (f) show the cyclone masks. The red lines shows the full track of the cyclones and the elongated oval masks the location of the cyclones at the analysis time

and 30 hours earlier. The mask captures Q_N surrounding the cyclone centres and along the trailing cold front. Sensitivity tests have been performed using a radial circle ranging from 12-16° and masks extending 24 to 36 hours prior to the analysis time.

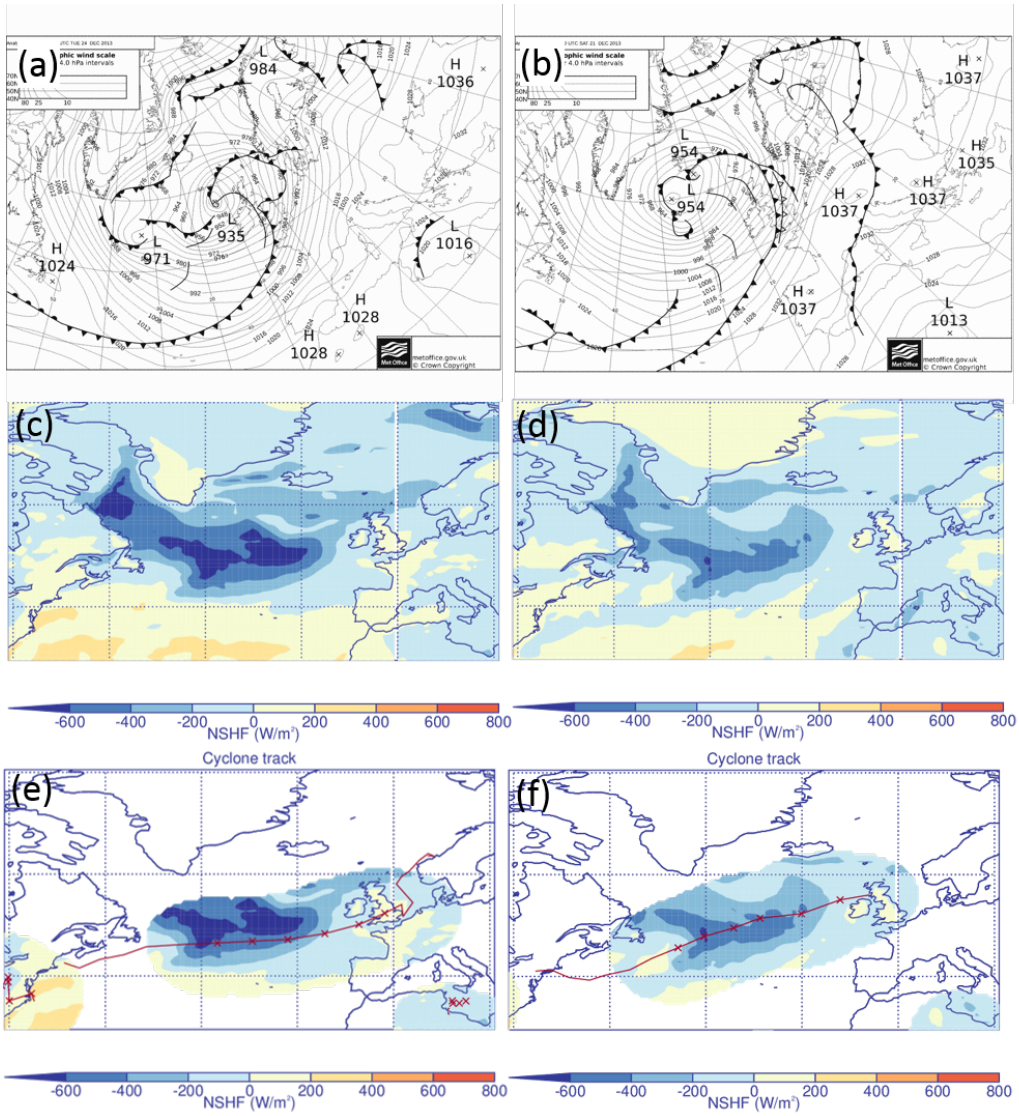

Figure 10. (a,b) UK Met Office synoptic analysis charts, (c,d) Q_N (W/m^2), (e,f) cyclone mask overlaid with tracks for (a,c,e) 00 UTC 24 December 2013 and (b,d,f) 00 UTC 20 December 2013. Red crosses show the position of cyclones at the analysis time and 30 hours previously.

4.1 2013/2014 SST anomalies

Figure 11(a) shows the 2013/2014 DJF SST tendency anomaly ($\Delta\text{SST}^{'}$) that is associated with anomalous Q_N. As expected $\Delta\text{SST}^{'}$ due to anomalous Q_N closely resembles the Q_N anomaly (shown in figure 9(f)) with anomalous cooling in the mid-North Atlantic where the flux anomaly is negative, and anomalous warming (less cooling than climatology) in the Gulf Stream and Norwegian sea regions. Small differences are due to spatial inhomogeneity in the North Atlantic climatological MLD. Figure 11(b) shows the 2013/2014 DJF $\Delta\text{SST}^{'}$ that is associated with anomalous MLD. The 2013/2014 MLD is shallower than the climatological average over much of the domain, particularly near the Gulf Stream region, and deeper than climatology in the mid-Atlantic region. In the mid-North Atlantic the enhanced negative Q_N results in negative buoyancy and thus mixing, deepening the MLD. Therefore, the surface flux decreases the temperature over a deeper layer of the ocean than usual, which reduces the direct SST cooling due to Q_N. At the same time, the increased MLD mixes colder water from below into the mixed layer which cools the surface indirectly. Figure 11(c) shows the sum of the $\Delta SST^{'}$ due to anomalous Q_N, anomalous MLD and anomalous entrainment ($\Delta SST^{'}_{ASI}$). It shows the same tripole pattern as the ΔSST_{TOT} anomaly (figure 11(d)) which has an average SST cooling anomaly of -1.0K in the mid-North Atlantic region (black box in figure 11(d)). The largest discrepancies occur along the east coast of North America suggesting that ocean dynamics are responsible for transporting warmer water into these regions via the western boundary currents. In the mid-North Atlantic region, the $\Delta SST^{'}_{ASI}$ accounts for 68% of the total anomalous SST cooling in the mid-North Atlantic.

4.2 2013/2014 cyclone and environmental flow SST anomalies

In this section we partition the Q_N anomaly into a part associated with the environmental flow (i.e., outside the cyclone masks described in section 2.6) and a part associated with the presence of cyclones (inside the cyclone masks described in section 2.6). Figure 12(a) shows the contribution to the DJF Q_N anomaly due to both cyclones and the environmental flow and figure 12(b) shows the contribution that is due to the environmental flow only. Both figures 12(a) and (b) show a tripole pattern with anomalously negative heat flux in between $40-60°$N and anomalously positive heat flux over the Gulf Stream and Norwegian Seas. This suggests that the overall pattern is controlled by the environmental flow. The anomalously positive heat flux in the Norwegian Sea and Gulf Stream region may be due to a reduced number of cold air outbreaks (Papritz and Spengler, 2017; Papritz and Grams, 2018; Parfitt et al., 2016). In the mid-north Atlantic the negative Q_N anomaly is enhanced, compared to contribution made by the environment (doubled from 32% to 68% of the total seasonal Q_N anomaly), when cyclones are present. In the Norwegian sea and Mediterranean sea the positive Q_N anomaly due to the environmental flow is suppressed by the presence of cyclones. Thus cyclones embedded within the environmental flow pattern tend to increase the negative surface heat flux, consistent with the cyclone-relative results in section 3.2. Varying the size of the cyclone mask radius from $12-16°$ results in a contribution to the total Q_N anomaly when cyclones are present in the mid-North Atlantic that ranges from $62-72\%$ and varying the length of the cyclone mask from $24-36$ hours results in a cyclone contribution from $62-71\%$. This suggests that the conclusion that cyclones enhance the Q_N anomaly does not depend strongly on the choices used to define the cyclone mask.

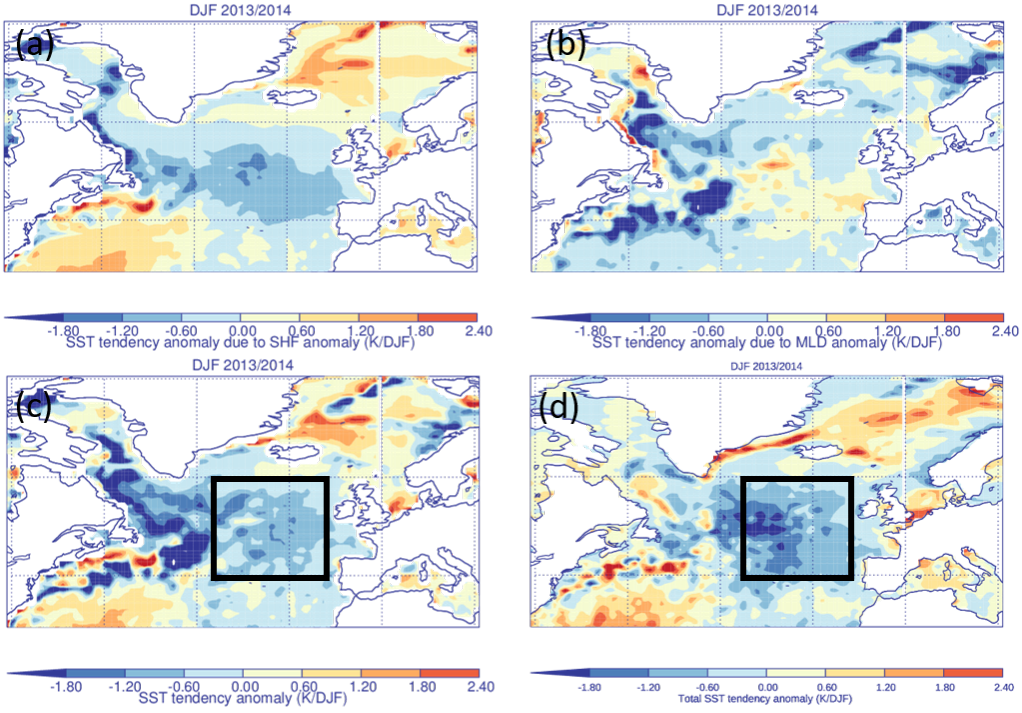

Figure 11. Anomalous ΔSST due to 2013/2014 (a) Q_N anomaly, (b) MLD anomaly and (c) ΔSST_{ASI} anomaly. (d) ΔSST_{TOT} anomaly.

Figure 12(c) shows the contribution to the 2013/2014 $\Delta SST'_{ASI}$ due to both cyclones and the environmental flow and figure 12(d) shows the contribution that is due to the environmental flow only. As for the Q_N anomaly, both show a tripole pattern suggesting that the environmental flow controls the anomalously large cooling in the mid-North Atlantic and the anomalously small cooling in the Norwegian Sea and Gulf Stream regions. In the mid-North Atlantic region, the negative $\Delta SST'_{ASI}$ is also enhanced (from 28% to 41% of the total seasonal $\Delta SST'$) when cyclones are present. This is less than their added contribution to the 2013/2014 Q_N anomaly because the enhanced negative Q_N is cooling a deeper layer of the ocean than usual which reduces the direct SST cooling.

5 Conclusions

In this paper we investigate both the SST cooling associated with individual cyclones and the SST cooling associated with the passage of multiple cyclones over the same location in the 2013/2014 season to determine how significant cyclones were in contributing to the anomalously large cooling that occurred during the 2013/2014 winter. We find that enhanced air-sea exchange of heat and moisture in the cold sector behind the cold front of an extratropical cyclone can lead to cooling of up to 0.2 K/day for the strongest cyclones. This cooling is relatively small compared to the variability in SST tendency in the North

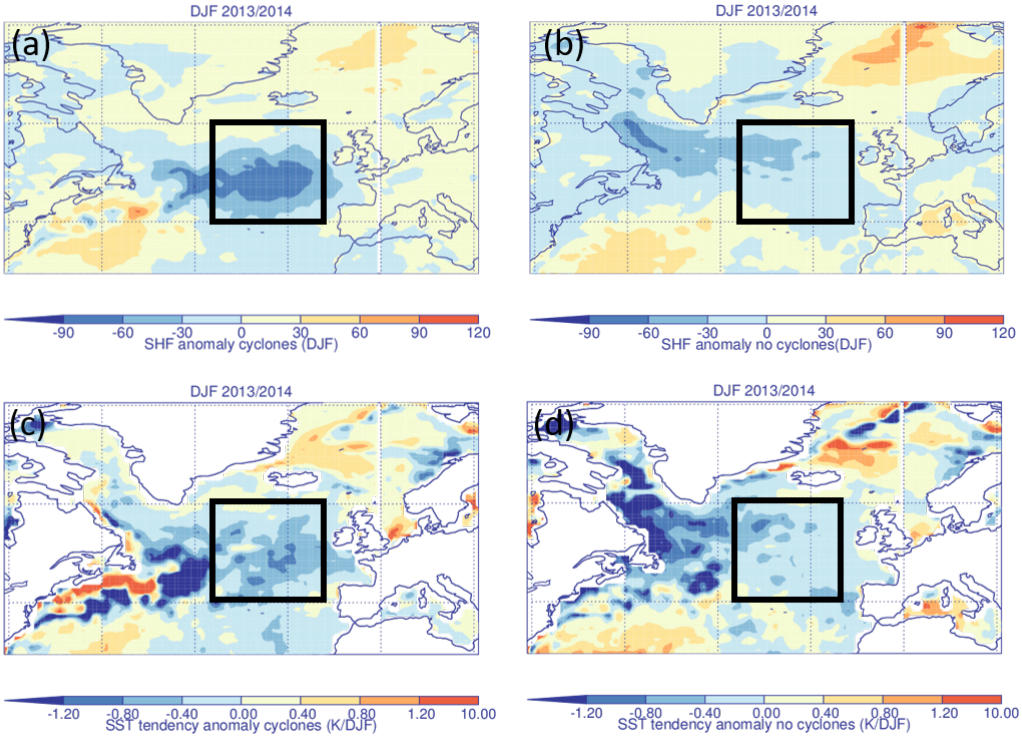

Figure 12. 2013/2014 anomalous Q_N associated with (a) both cyclones and the environmental flow and (b) the environmental flow. 2013/2014 anomalous ΔSST due to anomalous Q_N, MLD and entrainment associated with (c) both cyclones and the environmental flow and (d) the environmental flow.

Atlantic, thus the 'cold-wake' associated with the passage of an individual extratropical cyclone is difficult to observe in the instantaneous SST field.

320 During the 2013/2014 DJF season there was a zonal band of anomalously large negative heat fluxes extending from the east coast of the US towards Europe. The mixed layer depth was also anomalously deep in the mid-North Atlantic due to enhanced mixing and entrainment of water into the mixed layer from below. The combination of these air-sea interactions accounts for 68% of the total ΔSST anomaly. Thus air-sea interactions were very important in determining the anomalous SST cooling between December 2013 and February 2014.

325 In 2013/2014 the environmental flow pattern was anomalously zonal compared to climatology over the North Atlantic. This resulted in anomalously negative heat flux between $40-60°$N and anomalously positive heat flux over the Norwegian and Gulf Stream regions. When cyclones were present, heat flux from the ocean to the atmosphere was doubled in the mid-North Atlantic region. The enhancement of the negative heat flux caused a direct cooling of the ocean but also led to increased entrainment and thus a deeper mixed layer. This deepening reduces the overall effect of the cooling as the heat loss acts on a greater volume 330 of water than normal. Consequently, while the SST tendency anomaly in the mid-North Atlantic was enhanced by the presence

of cyclones it was by a smaller amount than might be expected due to a doubling of the heat flux. We conclude that both the environmental flow and extratropical cyclones embedded within this flow played important roles in determining the extreme 2013/2014 winter season SST cooling.

Author contributions. H.F.Dacre performed the data analysis for this publication. S.A.Josey and A.L.M.Grant contributed to the scientific interpretation of the analysis.

Competing interests. The authors declare that they have no conflict of interest.

Acknowledgements. The ERA-Interim data were obtained freely from http://apps.ecmwf.int/datasets/. The ORAS5 data were obtained freely from the Integrated Climate Data Center at University of Hamburg http://icdc.cen.uni-hamburg.de. Information on how to obtain the cyclone identification and tracking algorithm can be found from http://www.nerc-essc.ac.uk/ kih/TRACK/Track.html. We thank Kevin Hodges for providing his ETC tracking code. SJ receives funding from the UK Natural Environment Research Council including the ACSIS and EMERGENCE programmes.

References

Alexander, M. A. and Scott, J. D.: Surface flux variability over the North Pacific and North Atlantic oceans, Journal of climate, 10, 2963–2978, 1997.

Buckley, M. W., Ponte, R. M., Forget, G., and Heimbach, P.: Determining the origins of advective heat transport convergence variability in the North Atlantic, Journal of Climate, 28, 3943–3956, 2015.

Catto, J. L., Shaffrey, L. C., and Hodges, K. I.: Can climate models capture the structure of extratropical cyclones?, Journal of Climate, 23, 1621–1635, 2010.

Courtois, P., Hu, X., Pennelly, C., Spence, P., and Myers, P. G.: Mixed layer depth calculation in deep convection regions in ocean numerical models, Ocean Modelling, 120, 60–78, 2017.

Crawford, G. and Large, W.: A numerical investigation of resonant inertial response of the ocean to wind forcing, Journal of physical oceanography, 26, 873–891, 1996.

Dacre, H. F., Hawcroft, M. K., Stringer, M. A., and Hodges, K. I.: An extratropical cyclone atlas: A tool for illustrating cyclone structure and evolution characteristics, Bulletin of the American Meteorological Society, 93, 1497–1502, 2012.

Dacre, H. F., Martinez-Alvarado, O., and Mbengue, C. O.: Linking atmospheric rivers and warm conveyor belt airflows, Journal of Hydrometeorology, 2019.

Dee, D. P., Uppala, S., Simmons, A., Berrisford, P., Poli, P., Kobayashi, S., Andrae, U., Balmaseda, M., Balsamo, G., Bauer, d. P., et al.: The ERA-Interim reanalysis: Configuration and performance of the data assimilation system, Quarterly Journal of the royal meteorological society, 137, 553–597, 2011.

Fisher, E. L.: Hurricanes and the sea-surface temperature field, Journal of meteorology, 15, 328–333, 1958.

Grist, J. P., Josey, S. A., Jacobs, Z. L., Marsh, R., Sinha, B., and Van Sebille, E.: Extreme air–sea interaction over the North Atlantic subpolar gyre during the winter of 2013–2014 and its sub-surface legacy, Climate dynamics, 46, 4027–4045, 2016.

Hawcroft, M., Shaffrey, L., Hodges, K., and Dacre, H.: How much Northern Hemisphere precipitation is associated with extratropical cyclones?, Geophysical Research Letters, 39, 2012.

Hodges, K.: Feature tracking on the unit sphere, Monthly Weather Review, 123, 3458–3465, 1995.

Kawai, Y. and Wada, A.: Detection of cyclone-induced rapid increases in chlorophyll-a with sea surface cooling in the northwestern Pacific Ocean from a MODIS/SeaWiFS merged satellite chlorophyll product, International journal of remote sensing, 32, 9455–9471, 2011.

Kendon, M. and McCarthy, M.: The UK's wet and stormy winter of 2013/2014, Weather, 70, 40–47, 2015.

Kleinschmidt, E.: Principles of the theory of tropical cyclones, Arch. Meteor. Geophys. Bioklimatol, 4, 53–72, 1951.

Kobashi, F., Doi, H., and Iwasaka, N.: Sea surface cooling induced by extratropical cyclones in the subtropical North Pacific: Mechanism and interannual variability, Journal of Geophysical Research: Oceans, 124, 2179–2195, 2019.

Nelson, J., He, R., Warner, J. C., and Bane, J.: Air–sea interactions during strong winter extratropical storms, Ocean Dynamics, 64, 1233–1246, 2014.

Ogawa, F. and Spengler, T.: Prevailing Surface Wind Direction during Air-Sea Heat Exchange, Journal of Climate, 2019.

Papritz, L. and Grams, C. M.: Linking low-frequency large-scale circulation patterns to cold air outbreak formation in the northeastern North Atlantic, Geophysical Research Letters, 45, 2542–2553, 2018.

Papritz, L. and Spengler, T.: A Lagrangian climatology of wintertime cold air outbreaks in the Irminger and Nordic Seas and their role in shaping air–sea heat fluxes, Journal of Climate, 30, 2717–2737, 2017.

Papritz, L., Pfahl, S., Sodemann, H., and Wernli, H.: A climatology of cold air outbreaks and their impact on air–sea heat fluxes in the high-latitude South Pacific, Journal of Climate, 28, 342–364, 2015.

Parfitt, R., Czaja, A., Minobe, S., and Kuwano-Yoshida, A.: The atmospheric frontal response to SST perturbations in the Gulf Stream region, Geophysical Research Letters, 43, 2299–2306, 2016.

Parfitt, R., Czaja, A., and Kwon, Y.-O.: The impact of SST resolution change in the ERA-Interim reanalysis on wintertime Gulf Stream frontal air-sea interaction, Geophysical Research Letters, 44, 3246–3254, 2017.

Persson, G., Ola, P., Hare, J., Fairall, C., and Otto, W.: Air–sea interaction processes in warm and cold sectors of extratropical cyclonic storms observed during FASTEX, Quarterly Journal of the Royal Meteorological Society: A journal of the atmospheric sciences, applied meteorology and physical oceanography, 131, 877–912, 2005.

Pettersen, S., Bradbury, D. L., and Pedersen, K.: The Norwegian cyclone models in relation to heat and cold sources, Geophysica Norvegica, 1962.

Priestley, M. D., Pinto, J. G., Dacre, H. F., and Shaffrey, L. C.: The role of cyclone clustering during the stormy winter of 2013/2014, Weather, 72, 187–192, 2017.

Ren, X., Perrie, W., Long, Z., and Gyakum, J.: Atmosphere–ocean coupled dynamics of cyclones in the midlatitudes, Monthly weather review, 132, 2432–2451, 2004.

Rudeva, I. and Gulev, S. K.: Composite analysis of North Atlantic extratropical cyclones in NCEP–NCAR reanalysis data, Monthly Weather Review, 139, 1419–1446, 2011.

Schemm, S. and Sprenger, M.: Frontal-wave cyclogenesis in the North Atlantic–a climatological characterisation, Quarterly Journal of the Royal Meteorological Society, 141, 2989–3005, 2015.

Shaman, J., Samelson, R., and Skyllingstad, E.: Air–sea fluxes over the Gulf Stream region: Atmospheric controls and trends, Journal of Climate, 23, 2651–2670, 2010.

Sinclair, V. and Dacre, H.: Which Extratropical Cyclones Contribute Most to the Transport of Moisture in the Southern Hemisphere?, Journal of Geophysical Research: Atmospheres, 124, 2525–2545, 2019.

Stull, R. B.: An introduction to boundary layer meteorology, vol. 13, Springer, Dordrecht, 1988.

Tanimoto, Y., Nakamura, H., Kagimoto, T., and Yamane, S.: An active role of extratropical sea surface temperature anomalies in determining anomalous turbulent heat flux, Journal of Geophysical Research: Oceans, 108, 2003.

Toyoda, T., Fujii, Y., Kuragano, T., Kamachi, M., Ishikawa, Y., Masuda, S., Sato, K., Awaji, T., Hernandez, F., Ferry, N., et al.: Intercomparison and validation of the mixed layer depth fields of global ocean syntheses, Climate Dynamics, 49, 753–773, 2017.

Vannière, B., Czaja, A., Dacre, H., and Woollings, T.: A "cold path" for the Gulf Stream–troposphere connection, Journal of Climate, 30, 1363–1379, 2017.

Yao, Y., Perrie, W., Zhang, W., and Jiang, J.: Characteristics of atmosphere-ocean interactions along North Atlantic extratropical storm tracks, Journal of Geophysical Research: Atmospheres, 113, 2008.

Zolina, O. and Gulev, S. K.: Synoptic variability of ocean–atmosphere turbulent fluxes associated with atmospheric cyclones, Journal of climate, 16, 2717–2734, 2003.

Zuo, H., Balmaseda, M., de Boisseson, E., Hirahara, S., Chrust, M., and De Rosnay, P.: A generic ensemble generation scheme for data assimilation and ocean analysis, European Centre for Medium-Range Weather Forecasts, 2017.

Zuo, H., Balmaseda, M. A., Tietsche, S., Mogensen, K., and Mayer, M.: The ECMWF operational ensemble reanalysis–analysis system for ocean and sea ice: a description of the system and assessment, Ocean Science, 15, 779–808, 2019.

H. F. Dacre, S. A. Josey, A. L. M. Grant

December 20, 2019

Reply to reviewer 1

We would like to thank the reviewer for their comments on the paper. Below, the reviewers comments are in black and the responses in blue italics. Changes to the paper are shown in red in the revised paper.

General comment

The paper documents the sea surface cooling by extratropical cyclones and its impact on the 2013/2014 winter SST in the mid North Atlantic. The conclusions and interpretations are adequately supported for the most part. The paper is well written and conclusions are concise and clear.

Thank you.

Specific comments

1. Does the warming tendency in the warm sector has any effect on SST? In Section 4.1, the cyclone mask is created so as to encompass the cold front and the cyclone center. Does this method include the warm sector properly?
   The cyclone masking methodology was designed to capture the anomalous flux occurring behind the cold front and therefore the reviewer is correct, the effect of the warm sector (outside the 14° radius) is not assessed. This can be seen in the examples in figures 10(e) and (f) which capture the anomalously high flux behind the cold front but not the anomalously low flux ahead of the cold front (in the warm sector). However, it is also clear that the negative anomalies behind the cold front are 2-3 times larger in magnitude than the positive anomalies in the warm sector. We have tested the sensitivity of the results to increasing the mask radius to 16° and the contribution of cyclones to the total heat flux anomaly in the mid-north Atlantic increases from 68% to 71%. Therefore, making the mask larger, and thus including more of the warm sector, actually increases the contribution from cyclones. The results of the sensitivity test are already reported in the paper so we have not altered the text.

2. The authors focus on the 2013/2014 winter, but I expect that cyclones could play an important role even in other years. The authors might want to estimate cyclones contribution to the winter climatology of the net heat flux using your cyclone masking technique. It would develop a much deeper understanding of the cyclones role.

This is an excellent suggestion. We have started to apply our cyclone masking technique to other years and seasons. However, including this analysis would increase the length of the paper significantly. Therefore, we will publish this work as a separate publication to avoid a very long paper.

3. In addition to the strength and number of cyclones, the propagation speed is probably also important for the cooling. The high fraction of time of cyclone mask in 2013/2014 around the UK seems to be partly due to the stagnation of cyclones (Fig. 8).
The reviewer is right in their interpretation of the high mask fraction over the UK in the 2013/14 season. Towards the end of the storm track the cyclones slow down becoming quasi-stationary. The effect of propagation speed is taken into account in the masking methodology since multiple timesteps for a single cyclone will contribute to the seasonal climatological cyclone-related Q_N. This explanation has been added to section 4 of the revised paper.

4. Is the anomalously zonal storm track in 2013/2014 associated with the westerly jet?
Yes. As shown in Kendon et al. (2015), the 2013/14 season was associated with an anomalously strong and zonally elongated upper-level westerly jet. This extra information has been added to the text in section 4.

5. The distribution of the Qn anomaly in Figure 8f is different and shifted from that of the cyclones in Figure 8d. Why are they different?
As shown in figure 7, the maximum net surface heat flux occurs to the rear of the cyclone centre, typically to the north-west. Therefore, we expect the anomalous net surface heat flux to be to the north-west of the anomalous storm track activity.

6. The anomalous Qn not associated with cyclones in Figure 11b still has a tripole pattern. So do you think that the tripole pattern has basically nothing to do with cyclones?
This is an interesting point. Since the Q_N anomaly pattern when cyclones are not present is similar to that when cyclones are present we conclude that the environmental flow anomaly in 2013/2014 is responsible for generating the tripole of anomalous Q_N values. This pattern is consistent with the anomalous 500hPa geopotential height anomalies over the North Atlantic shown in Bao and Wallace (2015). The role of cyclones embedded within the seasonal flow anomaly is to enhance the negative Q_N anomalies in the mid-Atlantic and reduce the positive Q_N anomalies in the Norwegian Sea. We have re-written the description of this figure in section 4 to make the explanation clearer.

7. L153-164.rs It is difficult to identify the position of the cold front and warm section in Figure 4. How about plotting the cold and warm fronts? These fronts could be delineated based on Figure 5 or the map of relative vorticity of wind.
Cold and warm front position have been added to this figure.

Technical comments

1. L38. of the wind driven currents
Changed.

2. L128. over 6 K over the winter
   Changed

3. L135. The density of sea water 1000 kg/mˆ3 might be acceptable, but the more practical value (like 1024 kg/mˆ3) should be used.
   In the revised paper $1024 kg/m^3$ *has been used for the density of sea water. The conclusions remain unchanged.*

4. L143. figure 3(a)?
   Changed.

5. Figure 4. What do contour lines show?
   The contour lines show mslp. This has been added to figure 4 caption.

6. L246. the conclusion does not
   Changed.

7. L250. the anomalous Qn
   Changed.

8. L250. figure 8(f)
   Changed.

Kendon, M. and McCarthy, M., 2015. The UK's wet and stormy winter of 2013/2014. Weather, 70(2), pp.40-47.

Bao, M. and Wallace, J.M., 2015. Cluster analysis of Northern Hemisphere wintertime 500-hPa flow regimes during 1920–2014. Journal of the Atmospheric Sciences, 72(9), pp.3597-3608.

H. F. Dacre, S. A. Josey, A. L. M. Grant

December 20, 2019

Reply to reviewer 2

We would like to thank the reviewer for their comments on the paper. Below the reviewers comments are in black and the responses in blue italics. Changes to the paper are shown in red in the revised paper.

General comment

The paper explores a connection between SST anomalies and atmospheric cyclones in the North Atlantic. The paper is concise and well written.

Thank you.

My major concern is that the authors used a cyclone dataset, while their main finding relates more to cold fronts that are possibly associated with cyclones. I suggest adding a dataset on the location of fronts and calculating anomalies behind objectively identified cold fronts (perhaps within a cyclone area or independently) rather than deducing the location of fronts within cyclones.

See response to specific point 22.

Specific comments

1. Why only 2013/14 season is taken into account to calculate cumulative effect of the passage of multiple cyclones.There must be some other anomalous seasons.Tilinina et al. 2018 (https://doi.org/10.1175/MWR-D-17-0291.1) investigate anomalously high heat fluxes in the North Atlantic during winter and related those to the cyclone activity. They concluded that the area of interaction between cyclones and anticyclones is very important for a heat flux anomaly. I wonder if this is also true for the summer season and it will also be nice to see some analysis on this.
   This is an excellent suggestion and one that was also made by reviewer 1. We have started to apply our cyclone masking technique to other years and seasons. However, including this analysis would increase the length of the paper significantly. Therefore, we will publish this work as a separate publication to avoid a very long paper.

2. l. 3: are the processes not fully understood or not quantified?
   'Quantified' is probably more correct so we have changed the wording in the abstract.

3. l.29: I believe it should be Rudeva and Gulev (2011)
   We agree, this citation has been changed.

4. 5. l33: should it be left-rear quadrant?
   The SST cooling can be in either the right or left-rear part of the cyclone depending on the cold-front orientation. Therefore, this has been changed to 'rear part of the cyclone'.

5. l.41: I'd add 'ocean' surface mixed layer
   Changed.

6. l.89-92: you say 'MLD is the depth at which the density difference . . .. reaches 0.01 kg/m3' and then 'the density difference MLD can overestimate MLD'. Define MLD otherwise then.
   We have clarified that the overestimation of MLD using the density difference definition occurs predominantly in the deep convective regions and not over the entire North Atlantic domain. Since we focus on the mid-North Atlantic this does not influence our results.

7. l.98-100: 200 most intense cyclones - how does that number compare with the total number of cyclones for 1989-2009? How intense are those cyclones (perhaps, add a pdf intensity for all cyclones and those 200). As you focus on the North Atlantic, I'd suggest 30-70N, instead of 90N (though looking at the track in fig. 1 it will hardly make a difference for the results). Consider showing this area in Fig.1.
   Between DJF 1989/1990 and DJF 2008/2009 there were 1050 cyclones identified with their maximum intensity in the North Atlantic domain. The top 200 cyclones represent the top 19% of the entire North Atlantic distribution as shown in figure 1. We have decided not to include this figure, but have stated the percentage of the total cyclones in the text. As the reviewer states, the tracks of the most intense cyclones will not change if the North Atlantic domain is reduced along it's northern boundary, therefore we have not reanalysed the data.

8. l.105-113: How composites are built should be better described here. It is only in sec. 4.1 that we find out that the radius of composites is 30deg (it is also mentioned in fig 4 caption). I believe that the rotation of composites does not help interpretation of the results as meridional gradients in some plots get also rotated (e.g., fig. 4), I'd recommend skipping this step.
   We think that the reviewer must have missed this information, as it is stated in the first sentence of section 2.4 in which we describe the cyclone-relative compositing. Performing the rotation ensures that mesoscale features such as warm and cold fronts are approximately aligned and are not smoothed out by the compositing. We agree that this will also rotate meridional gradients, but feel that it is important to align the features we are interested in otherwise the composites become washed out. Therefore we have retained this step of the analysis.

9. l.111: Following your comment on the rate of intensification and decay, I think a pdf will be helpful (together with a pdf of intensity mentioned in my earlier comment)
   Dacre et al. (2012) (their figure 2(c)) shows the mean intensification and decay rates of the top 200 cyclones as well as the spread around the mean. As the pdf has already

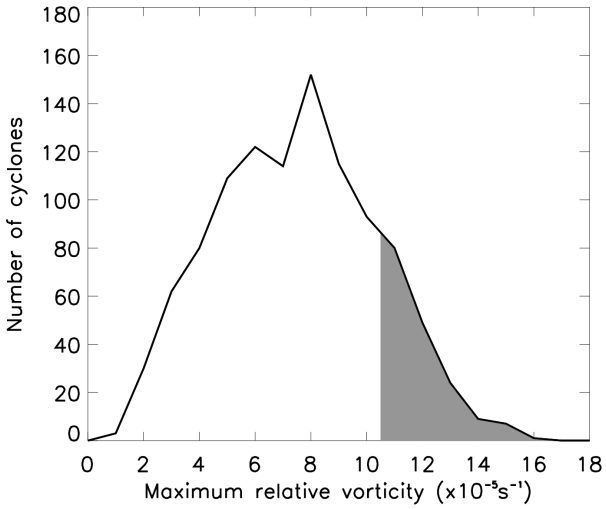

Figure 1: Maximum relative vorticity reached by all 1050 north Atlantic cyclones. The grey shading represents the part of the distribution that includes the 200 most intense cyclones.

been published we have not included it in this paper but have referred to the published figure in the revised text.

10. l.116: give a range for the meridional gradient
The meridional gradient is 50 $Wm^{-2}1000km^{-1}$. This has been added to the text.

11. Figures 1 and 2: Add Qsw,Qlw, etc. to the captions (as in other figures)
Added.

12. l.143: check the figure number
Corrected.

13. l.152: SST tendencies are discussed in the next section
Reference to SST tendency analysis has been removed.

14. l. 163: 'westward direction': as the composites are rotated it is hard to say where the west is.
'Westward direction' has been changed to 'behind the cyclone'

15. L 159:164: how much are sensible and latent heat fluxes in summer different to those in winter in previous studies (in Tilinina et al. 2018 and Rudeva and Gulev 2011)? From this you may possibly deduce a potential effect of cyclones on SST in winter (which can also be estimated directly in another paper)
We have not yet performed this analysis for any other seasons but this is a good suggestion and we will consider this in our future work.

16. l.165: this sentence suggests that wind should also be shown in fig 5b
The text about the winds now only refers to figure 5a.

17. Fig 3b and d: fix colours in the colour scale (blue - negative, yellow/red - positive)
We feel that the colourbar is clear so have not changed the figure.

18. Fig.4: I'd comment that positive values are into the surface in the caption.
This is already mentioned in the caption so we have not made any changes.

19. Fig.5: add 'air' to panel (a) caption
Added.

20. l.225-232: this paragraph should be in Methods
The section describing the cyclone masking has been moved to the methods section.

21. Fig.9: The relative sizes of the circles are wrong: if the big circle is 30 deg, as the small circle has a 14 deg radius.
The schematic has been re-drawn to better reflect the relative size of the circles.

22. l.237: I do not get why the mask shows the cyclone along the trailing cold front. It suggests that cold fronts always extend along the cyclone centres in the last 30 hours. If that is your assumption, that needs to be proved. As I said at the beginning of the review, I think you need objectively identified cold fronts instead of what has been invented here.
We have attempted to show that cold fronts roughly extend along the cyclone centres in the last 30 hours by showing 2 examples of the masking application in figure 10. We decided to use a cyclone tracking algorithm rather than a cold front tracking algorithm because it is the advection of cold dry air behind the cold front which creates the anomalous surface flux. Identifying relatively cold and/or dry airmasses without the co-location with cyclonic winds would not result in large heat flux.

23. Fig 10: Maybe swap the panels to have 24 Dec on the right and 20 Dec on the left
We are unsure why changing the ordering of the figure would improve the clarity of the paper so we have not swapped the panels around.

24. l.245: 14-18% - what variable does it relate to?
Following modifications to the text in response to other comments this sentence has been removed.

25. l249, 250 : fig 11c and 8f, respectively
We have changed the figure references.

26. Fig11: perhaps I missed it, but was QN due to cyclones calculated for all cyclones in 2013/14, or the strongest? Fig. 11c shows SSTQN due to cyclones or any Qn? I think 11c should be due to cyclones only. Can you explain why strong negative anomalies in the west of the North Atlantic (fig. 11c) are not seen in fig. 11d? I'd say that 11d matches well with 11a, which makes sense, but anomalies in the west North Atlantic in 11d are confusing
To clarify, Q_N in figure 11(a) was due to all cyclones in 2013/2014 not just the strongest.

Figure 11(c) showed ΔSST_{QN} due to the total Q_N anomaly combined with the climatological MLD. In response to a comment from reviewer 3 we now use the monthly varying MLD for 2013/2014.
The SST tendency anomaly for the 2013/2014 season is determined by subtracting the climatological SST tendency from the 2013/2014 SST tendency. The SST tendency anomaly can be separated into the anomaly associated with (i) anomalous Q_N (term 1 in equation 1), (ii) anomalous MLD (term 2 in equation 1) and (iii) anomalous entrainment through the base of the mixed layer, Q_{ENT} (term 3 in equation 1). We refer to the sum of these quantities as the SST tendency anomaly due to air-sea interactions (ASI), $\Delta SST'_{ASI}$, given by;

$$\Delta SST'_{ASI} = \frac{Q^i_N - \overline{Q_N}}{\rho c_p \overline{h}} + \frac{Q^i_N}{\rho c_p}\left(\frac{1}{h^i} - \frac{1}{\overline{h}}\right) + \frac{Q^i_{ENT} - \overline{Q_{ENT}}}{\rho c_p \overline{h}}, \quad (1)$$

where i represents the 2013/2014 values and the overbar represents the 1989-2015 climatological values. Since we have no measurements of the entrainment flux anomaly across the ocean boundary layer it is estimated to be 20% of the surface Q_N anomaly (Stull (1988)). Neglecting contributions made by wind driven turbulence.
$\Delta SST'$ due to anomalous Q_N is shown in figure 2(a). This closely resembles the Q_N anomaly (figure 11a in the original paper) with anomalous cooling in the mid-North Atlantic where the flux are negative, and anomalous warming (less cooling than climatology) in the Gulf Stream and Norwegian Sea regions. $\Delta SST'$ due to anomalous MLD is shown in figure 2(b). This has the opposite pattern to figure 2(a) since larger negative Q_N results in deepening of the MLD via mixing by negatively buoyant water. Thus the large $\Delta SST'$ in the west-North Atlantic are the result of the MLD being anomalously shallow in the 2013/2014 season. The sum, $\Delta SST'_{ASI}$, accounts for 68% of the total $\Delta SST'_{TOT}$ in 2013/2014.

We have also calculated both Q_N and $\Delta SST'_{ASI}$ due to the environmental flow and when cyclones are present. Cyclones embedded within the environmental flow are associated with 68% of the total Q_N anomaly, more than double the Q_N due to the environmental flow anomaly only (32%). However, due to significant compensation between $\Delta SST'$ due to anomalous Q_N (figure 3(a)) and $\Delta SST'$ due to anomalous MLD (figure 3(c)) the $\Delta SST'_{ASI}$ when cyclones are present (figure 3(e)) accounts for 41% of the observed ΔSST compared to 28% when cyclones are not present. Sections 4.1 and 4.2 have been re-written to clarify these points.

27. l.255: is it entrainment of the cold air?
This sentence refers to the entrainment of cold water into the ocean mixed layer from below. This has been clarified in the text.

28. l.265: As the mask stretches backwards from the cyclone centre, it captures the cold sector. However, the effect of the warm sector remains not assessed (which can also be done if warm fronts are identified).
The cyclone masking methodology was designed to capture the anomalous flux occurring behind the cold front and therefore the reviewer is correct, the effect of the warm sector

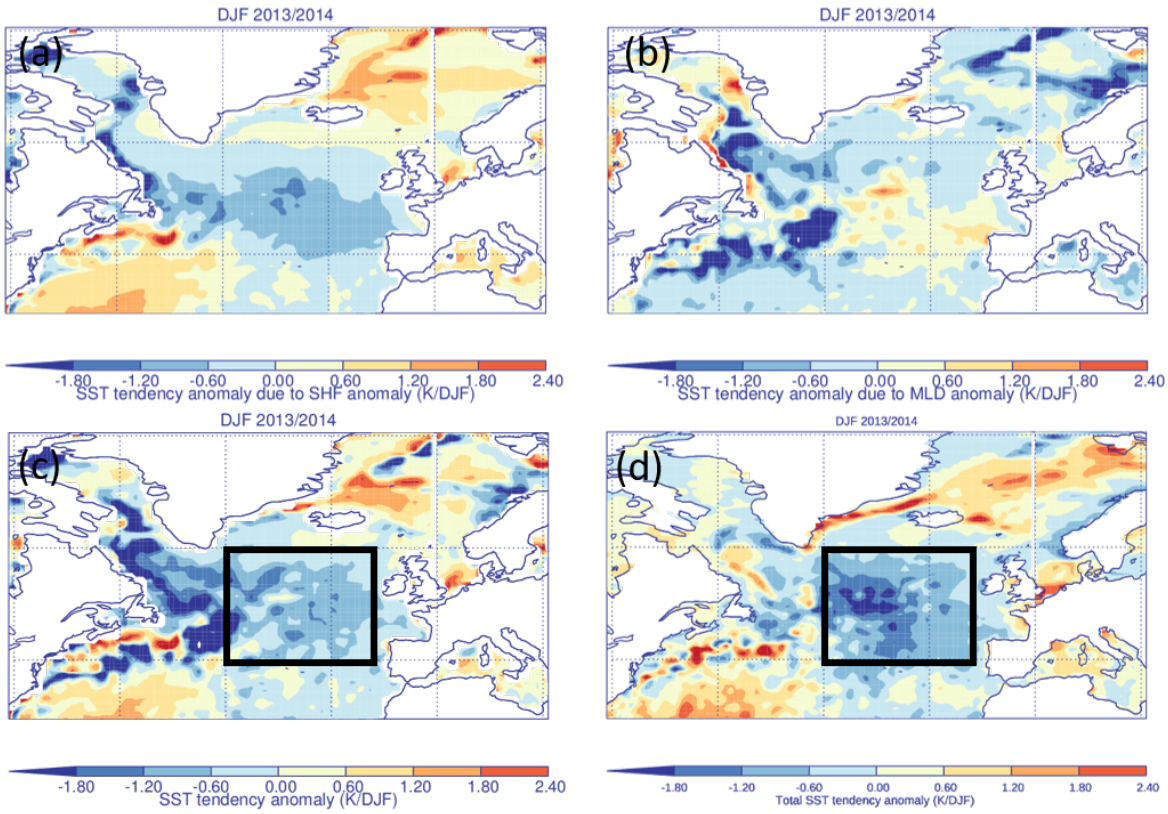

Figure 2: Anomalous SST tendency due to 2013/2014 (a) Q_N anomaly, (b) MLD anomaly and (c) Q_N, MLD and entrainment anomaly. (d) Total SST tendency anomaly.

(outside the 14° radius) is not assessed. This can be seen in the examples in figures 10(e) and (f) which capture the anomalously high flux behind the cold front but not the anomalously low flux ahead of the cold front (in the warm sector). However, it is also clear that the negative anomalies behind the cold front are 2-3 times larger in magnitude than the positive anomalies in the warm sector. We have tested the sensitivity of the results to increasing the mask radius to 16° and the contribution of cyclones to the total heat flux anomaly in the mid-north Atlantic increases from 68% to 71%. Therefore, making the mask larger, and thus including more of the warm sector, actually increases the contribution from cyclones. The results of the sensitivity test are already reported in the paper so we have not altered the text.

29. Fig. 7 suggests that the warm sector will have relatively small effect during the max development, but at other stages of cyclone lifecycles the balance might be different. *Figure 7 shows the SST change due to Q_N only at 3 stages in the cyclone lifecycle (max*

-24, max and max +24). We have also analysed the SST changes at max -48 and max -36. The effect of the warm sector appears to reduce during these very early stages of cyclone development.

Technical comments

1. The word 'flux' is often used in plural form (e.g., flux occur). My preference is either to say 'flux occurs' or 'fluxes occur'.
   We have changed 'flux occur' to 'flux occurs' throughout the paper.

2. l. 73: magnitudes
   Corrected.

3. l.101: position is
   As cyclones is plural, we think that position 'are' rather than 'is' the correct wording.

4. l.126, 166,173: Figure shows
   As figure is singular, we think that 'show' rather than 'shows' in the correct wording on these lines.

5. l.128: 'teh' to 'the'
   Corrected.

6. l.135: put comma after 4000Jkg-1K-1
   Corrected.

7. l. 137: change 10's to 10s
   Corrected.

8. l.147: remove 'are'
   Removed.

9. Fig 7: 'Normalised' and 'negative' should start with a small letter
   Corrected.

10. l.246: remove 'is'
    Removed.

Stull R.B. (1988) Convective Mixed Layer. In: Stull R.B. (eds) An Introduction to Boundary Layer Meteorology. Atmospheric Sciences Library, vol 13. Springer, Dordrecht

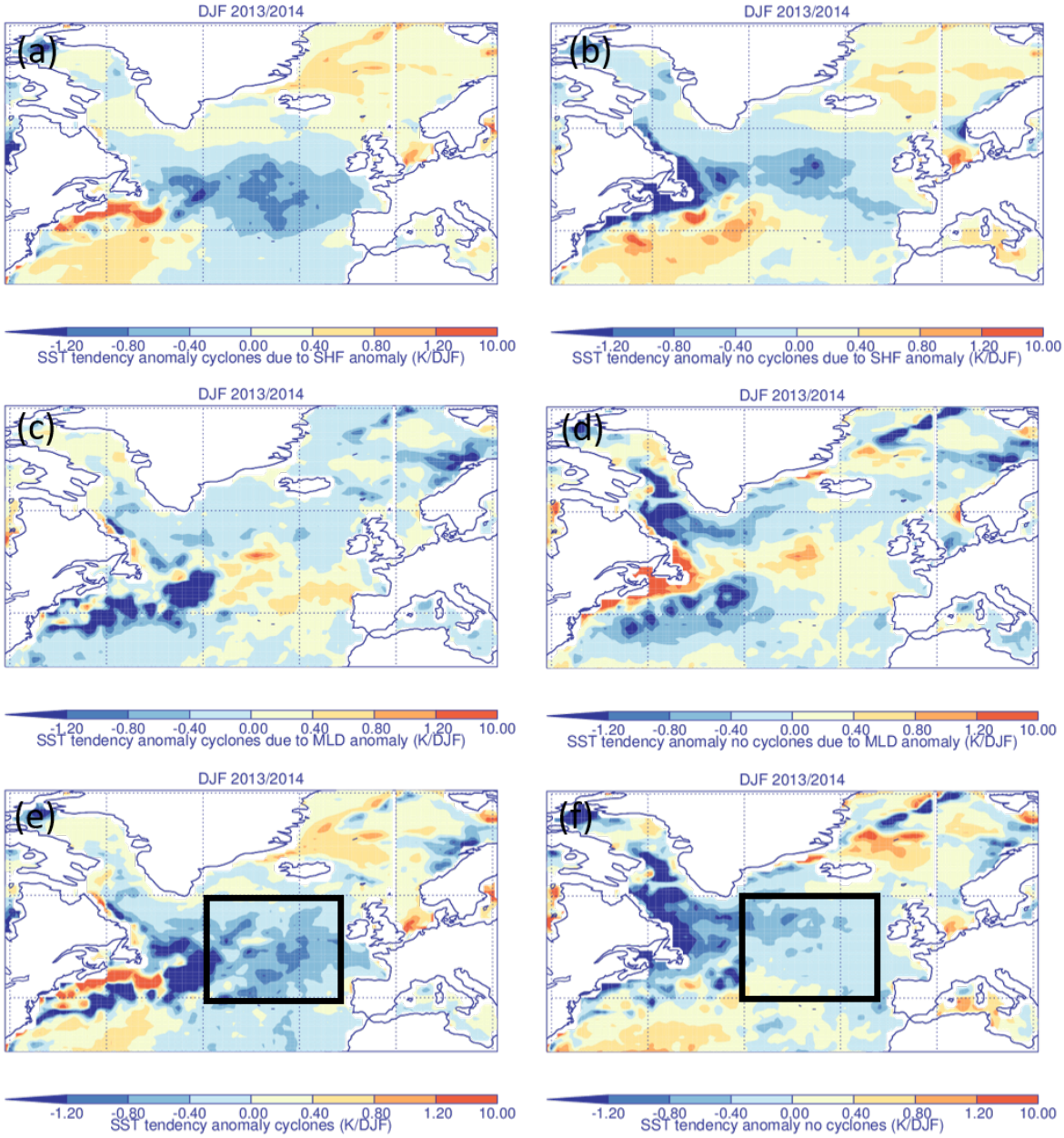

Figure 3: 2013/2014 anomalous SST tendency associated with (a) Q_N anomaly due to cyclones, (b) Q_N anomaly due to not associated with cyclones, (c) MLD anomaly when cyclones present, (d) MLD anomaly when cyclones not present, (e) sum of Q_N, MLD and entrainment anomalies when cyclones present and (f) sum of Q_N, MLD and entrainment anomalies when cyclones not present.

H. F. Dacre, S. A. Josey, A. L. M. Grant

December 20, 2019

Reply to reviewer 3

I would like to thank the reviewer for their comments on the paper. Below the reviewers comments are in black and the responses in blue italics. Changes to the paper are shown in red in the revised paper.

General comment

The Authors present an interesting analysis using ERA-Interim data to address the question how extratropical cyclones influence the SST in the Atlantic. They showcase one particular year that featured a significant SST anomaly and try to attribute a large fraction of this anomaly to anomalous cyclone activity in the same winter. The manuscript is well written and the figures are clear, though the panel labels are sometimes difficult to see as they are on top of shaded figures. Overall, the paper presents a valuable contribution to the field and employs a novel diagnostic to attribute the surface fluxes to individual cyclones.

Thank you.

However, there are several points in the paper that need further clarification, which are indicated in the comments below.

Specific comments

1. The mixed layer calculation has a caveat, because the authors assume that the depth has no variations throughout the year when they make seasonal budgets. One particular issue with that is that as the mixed layer depth changes, the sea state properties, in particular the stratification below the mixed layer, become important when the mixed layer depth increases. The actual heat content in the mixed layer will depend on the sea state below the mixed layer as well when net surface flux causes mixing. The entrainment of sea water below the column would need to be considered when the fluxes imply a net change in mixed layer depth. It would thus be interesting if the authors also show the seasonal tendency of the mixed layer depth in figure 3, not only the tendency in SST. Given the actual change of mixed layer depth together with the ocean stratification below the mixed layer could yield an estimate of the entrained energy into the changed mixed layer from below. This additional term in the heat budget could be accounted for and contrasted with the net surface forcing of the SST tendency.

   Figure 1 shows the climatological MLD and MLD seasonal tendency. The MLD and

MLD tendency patterns are very similar with greatest deepening of the mixed layer occurring where the average MLD is deepest. We have not added the additional figure to the paper but added that 'On average the MLD deepens by 50% between December and February outside the deep convection regions' to the paper text.

The reviewer is correct that the entrainment of sea water at the base of the ocean mixed layer is important. Figure 2(a) shows the 2013/2014 SST tendency anomaly, $\Delta SST'$, that is associated with anomalous Q_N. As expected $\Delta SST'$ due to anomalous Q_N closely resembles the Q_N anomaly (shown in figure 9(f) in paper) with anomalous cooling in the mid-North Atlantic where the flux are negative, and anomalous warming (less cooling than climatology) in the Gulf Stream and Norwegian sea regions. Small differences are due to spatial inhomogeneity in the North Atlantic climatological MLD. Figure 2(b) shows the 2013/2014 $\Delta SST'$ that is associated with anomalous MLD. The 2013/2014 MLD is shallower than the climatological average over much of the domain, particularly near the Gulf Stream region, and deeper than climatology in the mid-Atlantic region. In the mid-North Atlantic the enhanced negative Q_N results in negative buoyancy and mixing, deepening the MLD. Thus, the surface flux decreases the temperature over a deeper layer of the ocean than usual which reduces the direct SST cooling due to Q_N. At the same time, the increased MLD entrains colder water at the base of the ocean mixed layer which cools the surface indirectly. This effect is estimated to be 20% of the Q_N anomaly (Stull, 2012). Neglecting contributinos made by wind driven turbulence. Figure 2(c) shows the sum of the SST tendency anomaly due to anomalous Q_N, MLD and entrainment (referred to as the SST tendency anomaly due to air-sea interactions in the paper, $\Delta SST'_{ASI}$). It shows the same tripole pattern as the $\Delta SST'_{TOT}$ (figure 2(d)) which has an average SST cooling amomaly of -1.0K in the mid-North Atlantic region (black box in figures 2(d)). The largest discrepancies occur along the east coast of North America suggesting that ocean dynamics is responsible for transporting warmer water into these regions via the western boundary currents. In the mid-North Atlantic region, the $\Delta SST'_{ASI}$ accounts for 68% of the observed anomalous cooling in the mid-North Atlantic. This figure and explanation has been added to the paper.

2. Regarding the methodology of cyclone frequency, it is not clear if every cyclone is counted multiple times for the track densities of if some kind of anti-aliasing was employed. This would also influence how storm track activity is defined, as fewer but slower moving storms would yield a higher storm activity in terms of cyclone density compared to the same number of cyclones in a season with hizher phase velocity. It would be great if the authors could further clarify how the cyclone track densities were calculated and how exactly one can thus understand an increased activity of cyclones. It would also be of interest if there were more extreme cyclones that particular year of interest, especially as the authors limit their analysis to the more intense systems.
In this paper the effect of propagation speed is taken into account in the masking methodolgy since multiple timesteps for a single cyclone contribute to the seasonal climatological cyclone-related Q_N. As a result, the high mask fraction over the UK in the 2013/14 season occurred because there were both a higher than average number of cy-

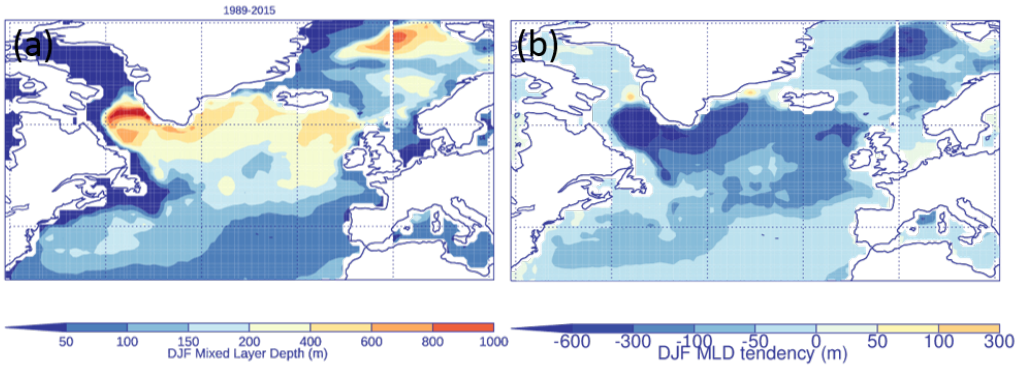

Figure 1: North Atlantic DJF 1989-2015 (a) mixed layer depth and (b) mixed layer depth seasonal tendency (m).

clones and because the cyclones slowed down becoming quasi-stationary over the UK. This clarification of the methodology has been added to the text. The analysis for the 2013/2014 season is not limited to intense cyclones as all cyclones are considered.

3. A large fraction of the fluxes in the Gulf Stream region are associated with cold air outbreaks, of which a significant fraction is not necessarily associated with cyclones in the storm track region. Could the reduced QN fluxes in 2013/2014 south of the Gulf Stream region as well as in the Nordic Seas be thus actually associated with a reduced number of cold air outbreaks? For the Nordic seas, which also feature a significant anomaly in the presented analysis, Papritz and Spengler (J. Clim., 2017) showed that cold air outbreaks account for the larges fraction of the surface fluxes in this region. Thus, the apparent anomalies are most likely mainly attributable to variations in cold air outbreaks and maybe only indirectly or in a reduced way associated with extra-tropical cyclones. Papritz and Grams (GRL, 2018) investigated the weather regimes associated with cold air outbreaks in the region of interest in the manuscript at hand. It would be interesting to put their findings and the given role of cold air outbreaks on the surface fluxes in the region in context with the presented findings.
It is possible that the reduced Q_N flux in the Gulf Stream region and in the Nordic Seas are associated with cold air outbreaks. Indeed, in the revised version of the paper we attribute these positive heat flux anomalies to the environmental flow pattern which was anomalously zonal, potentially reducing cold air outbreaks. Therefore we have added this explanation to the paper and referenced the papers suggested.

4. In addition to cold air outbreaks, the role of cold fronts for surface fluxes in the Gulf Stream region has also been discussed recently, e.g., Parfitt and Czaja (2016) and other recent studies by the first author. It would be great if the authors could provide further context of the presented work to these studies.
Since we have focussed our analysis on the mid-North Atlantic region and not the Gulf Stream we have not included a detailed discussion of the relationship between this work and that presented by Parfitt and Czaja (2016). However, in future studies we will extend this work to other regions so we thank the reviewer for this reference.

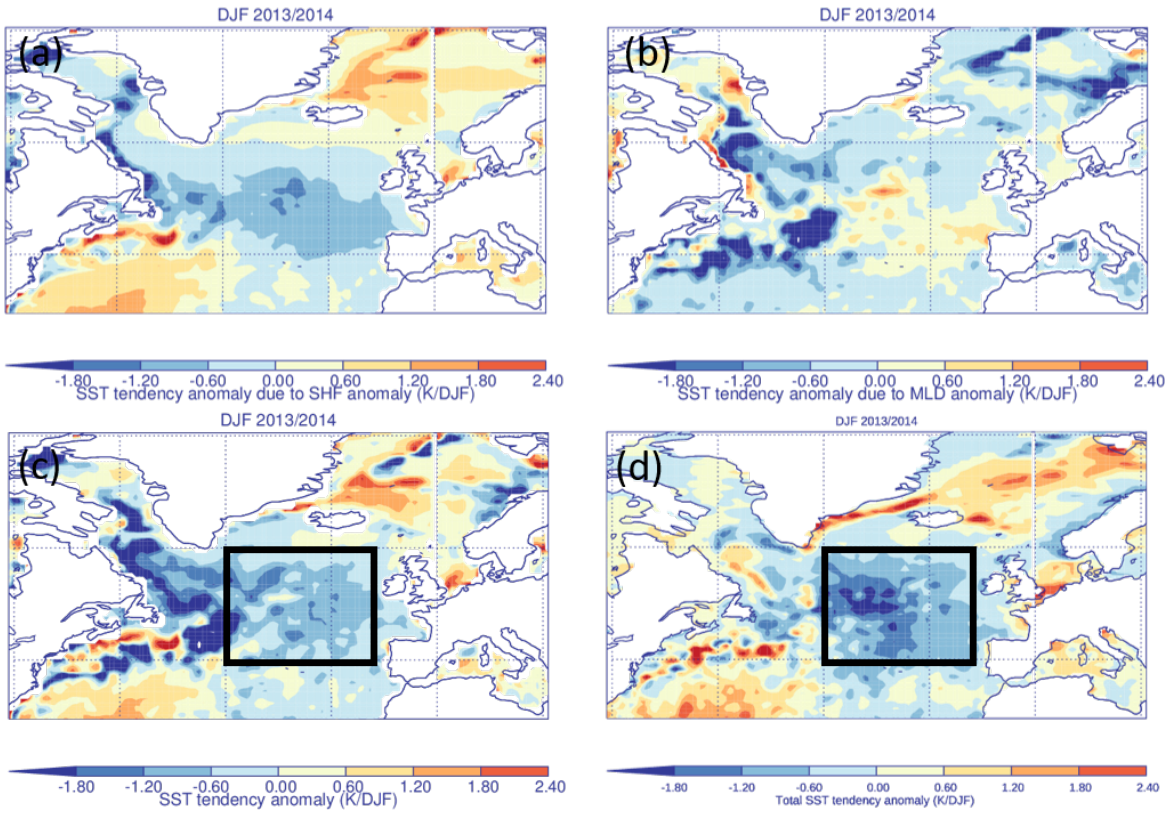

Figure 2: $\Delta SST'$ due to 2013/2014 (a) Q_N anomaly, (b) MLD anomaly and (c) air-sea interaction anomaly. (d) $DeltaSST'_{TOT}$.

5. The method to define the QN with the cyclone masks is not clear enough. It is difficult to follow what is actually summed up. At each time t for a given cyclone, the position of the cyclone and the preceding 30 hours positions are used, but is this done for every timestep in the cyclone evolution? How would this differ to just taking the swath with circles around all cyclone positions along the entire cyclone track? It would be great if the authors could provide further details about the employed method.
The reviewer is correct. The mask method is performed for every timestep in the cyclone evolution, which is equivalent to taking a swath with circles around all positions along the cyclone track, but only the track in the preceeding 30 hours, not the entire length of the track. We have made this method clearer in the revised paper.

Technical comments

1. P1 L7: The connection between the "cold wake" and "climatological variability" is not quite clear in this sentence. How is the size of the cold wake associated to climatological

variability?
Here we specifically refer to climatological variability in the SSTs. We have clarified this in the text.

2. P1 L21: The argument about the role of cold fronts has also been discussed more recently, e.g., Parfitt and Czaja (2016) and other recent studies by the first author. What is the context of the presented work to these studies?
Links to more recent work is made in the introduction (lines 46 onwards). We have added a reference to Parfitt and Czaja (2016) in this section.

3. P2 L29: After citing the study by Zolina and Gulev (2003), the reader is a bit confused about the thus far identified fluxes associated with extratropical cyclones. If there is a controversy, it would be great if the authors could further highlight these conflicting results and possibly indicate as to why they are conflicting or if they will address these contrasting results.
We have expanded the description of the results in this paper which suggest at least partial cancellation of the flux anomalies associated with cyclones.

4. P2 L28" . . . of the wind driven. . .
Corrected.

5. P2 L44: The authors comment on the role of ocean dynamics in the western Pacific, where oceanic advection probably plays a dominant role. However, the reader is left wondering if not similar arguments would also apply to the western Atlantic, the focus of this study, where strong oceanic currents are present. Are there no studies quantifying the role of oceanic anomalies in the western Atlantic? Good if the authors can also comment on the region of their interest in this context.
We have included a reference to Buckley et al. (2015) who also find that in the Gulf Stream region, ocean dynamics are important in setting the upper-ocean heat content anomalies on interannual time scales and that air–sea heat flux damp anomalies created by the ocean.

6. P2 L51: Another, more direct, connection between cold air outbreaks, cyclones, and the low-level baroclinicity in the western Atlantic is provided by Papritz and Spengler (2015) as well as Vanniere et al. (QJ, 2017).
Papritz and Spengler (2015) is cited in the previous sentence so we have not added a further citation here.

7. P5 L128: "the winter"
Corrected.

8. P7 L140: See general comment about change of mixed layer depth throughout season. Some additional discussion about the influence of mixing and entrainment in the ocean would be valuable.
See response to general comment 1.

9. P7 L144: "heat fluxes occur"
Changed to 'heat flux occurs'.

10. P7 L147-149: This is also the argument of a recent study by Ogawa and Spengler (2019), who also emphasized the role of synoptic eddies on the climatological fluxed in the mid and higher latitudes.
Thank you for this reference, we were not aware of this paper. A citation to this work has been added.

11. P9 L183: "the cyclone lifecycle"
Corrected.

12. P11 L203: "the surface flux"
Corrected.

13. P12 L216: It is not necessarily obvious from the referenced figures that the storm track was more active, see general comment on cyclone track densities.
See response to specific comment 2.

14. P13 L223: It is difficult to see how the QN anomaly and the storm track anomaly is "consistent". There appear to be more cyclones detected over the Gulf Stream region in the anomalous winter, though the net negative QN fluxes in this region appear to be reduced when compared to climatology. How can this be reconciled with the previous findings of the cyclone relative QN fluxes and SST changes?
We agree that the relationship between the Q_N anomaly and storm track anomaly is not clear close to the continental regions where ocean dynamics are dominant. For this reason we have chosen to focus on the mid-Atlantic region only in the paper. We have re-written the text to emphasise that the anomaly in the mid-Atlantic region is consistent with the shift in the storm track, with cyclones travelling more zonally from the US towards western Europe rather than north-eastwards towards Iceland.

15. P14 L225 and following: The methodology is not quite clear, see also general comments.
See response to general comment 2.

16. Fig. 9 caption: "red crosses show"
Corrected.

17. P15 L246: "conclusion does not"
Corrected.

18. P16 L250: It is not clear that the results indicated in this paragraph consider the data based on the cyclone swaths from the previous section.
We have re-written this section of the paper to respond to comments from reviewer 2.

19. P16 L254: The actual percentage of the SST difference cannot be really directly contributed to the fluxes, as it is a mix of local fluxes and advection, as well as entrainment from below that caused the total change. There can be compensating effects that cannot be accounted for in such a crude attribution without actually calculating a full budget considering all tendency terms.
We agree that several factors contribute to the SST tendency anomaly and that they might be compensating. We have estimated the SST tendency anomaly due to (i)

anomalous Q_N , (ii) anomalous MLD and (iii) anomalous entrainment. Therefore, we have performed a more complete analysis of the air-sea interactions and indeed there are compensating effects which are now described in the revised paper.

20. P17 L262: Can the authors comment further on the relative contributions of potential other effects that make the attribution to individual cyclones difficult?
We have decomposed the total SST tendency anomaly due to Q_N into three components (see figure 1). We have attributed the difference between the sum of these components (referred to as air-sea interactions) and the total SST tendency anomaly to be due to advection. We note that there are significant assumptions in this method but are confident that the main conclusion that cyclones enhance SST cooling in the mid-North Atlantic region is robust.

21. P17 L266: The statement about "higher than average cooling" appears to be rather regionally confined and there were also larger areas where this particular season featured reduced air-sea heat exchange. The authors should comment on this complex structure and put it in context to the observed cyclone distribution. Especially the western Atlantic area with reduced fluxes appears difficult to explain given the increased number of cyclones (Fig. 8f, 11d).
Over almost the entire domain cyclones decrease the SSTs. The reduced air-sea heat exchange over the Gulf Stream and Norwegian Sea is controlled by the environmental flow anomaly. This explanation has been added to the paper text.

Buckley, M.W., R.M. Ponte, G. Forget, and P. Heimbach, 2015: Determining the Origins of Advective Heat Transport Convergence Variability in the North Atlantic. J. Climate, 28, 3943–3956, https://doi.org/10.1175/JCLI-D-14-00579.1

Stull R.B. (1988) Convective Mixed Layer. In: Stull R.B. (eds) An Introduction to Boundary Layer Meteorology. Atmospheric Sciences Library, vol 13. Springer, Dordrecht